Transport of substrate and biomass in a packed bed bioreactor
by Ross Wade Lundman

A thesis submitted in partial fulfillment .of the requirements for the degree of Master of Science in Chemical Engineering
Montana State University

Abstract:
Packed bed or porous media type systems are a unique environment for bacterial growth. The large surface areas, plug flow mixing, and laminar hydrodynamics may offer the attached organisms higher nutrient concentrations at lower shear stresses when compared to regimes such as plug, laminar, or completely mixed flows. Industries affected by biological accumulations in porous media range from oil recovery to waste water treatment. Perspective may be the only factor in deciding whether such an accumulation is useful or detrimental.

As industry has become more aware of the importance of such accumulations, more emphasis has been placed upon modelling the affected systems. Two areas where modelling has suffered from a lack of data are cellular detachment rates and substrate transport. The objectives of this research were 1) correlation of cellular detachment rate with glucose utilization rate and 2) observation of changes in transport of dissolved components through the porous media as a result of the biological accumulation.

To accomplish these objectives, two series of experiments were run. A differential reactor was packed with 1-mm glass beads, inoculated with Pseudomonas aeruginosa, and operated at a constant flow rate. In the first series of experiments the inlet glucose concentration was 18 g m"3. In the second series of experiments the glucose concentration was lowered to 2 g m-3. This change in influent glucose concentration provided for a wide range of accumulation rates and glucose utilization rates. Cell concentrations and glucose concentrations were measured daily at the influent and effluent of the reactor. Stimulus-response studies were also performed daily.

Results indicated detachment rate was a function of glucose utilization rate. Theory suggested the correlation may be linear; however, noise in the data made this determination impossible. The stimulus-response studies demonstrated the strong dependence of mixing characteristics upon the extent of the biological accumulation.

TRANSPORT OF SUBSTRATE AND BIOMASS IN A PACKED BED BIOREACTOR

by

Ross Wade Lundman

A thesis submitted in partial fulfillment
of the requirements for the degree

of

Master of Science

in

Chemical Engineering

MONTANA STATE UNIVERSITY
Bozeman, Montana

December 1992

APPROVAL

of a thesis submitted by

Ross Wade Lundman

This thesis has been read by each member of the thesis committee and has been found to be satisfactory regarding content, English usage, format, citations, bibliographic style, and consistency, and is ready for submission to the College of Graduate Studies.

1/26/93
Date

Ronald W. Lasen
Chairperson, Graduate Committee

Approved for the Major Department

1/26/93
Date

Head, Major Department

Approved for the College of Graduate Studies

2/3/93
Date

Graduate Dean

STATEMENT OF PERMISSION TO USE

In presenting this thesis in partial fulfillment of the requirements for a master's degree at Montana State University, I agree that the Library shall make it available to borrowers under rules of the Library.

If I have indicated my intention to copyright this thesis by including a copyright notice page, copying is allowable only for scholarly purposes, consistent with "fair use" as prescribed in the U.S. Copyright Law. Requests for permission for extended quotation from or reproduction of this thesis in whole or in parts may be granted only by the copyright holder.

Signature Ron W Lendsman

Date 1-24-93

ACKNOWLEDGEMENTS

The author acknowledges the Center for Interfacial Microbial Process Engineering at Montana State University (a National Science Foundation Engineering Research Center) and the Center's Industrial Associates. Although the research has been funded in part by the U.S. Environmental Protection Agency under Assistance Agreement R-815709 to Montana State University through the Hazardous Substance Research Center for U.S. regions 7 and 8 headquartered at Kansas State University, it has not been subjected to the Agency's peer and administrative review and, therefore, may not necessarily reflect the views of the Agency, and no official endorsement should be inferred.

I am indebted above all to my academic advisor, Ronald Larsen, who donated endless hours of labor and consultation. Likewise, a great debt is owed to my research advisor, Al Cunningham, for providing advice and funding. Thanks are also due to Warren Jones and John Sears for their contributions as committee members.

Among other students and staff, I would like to thank Judith Baker, Bill Drury, Brian Goldstein, Thomas Griebe, Jason Hayes, WhonChee Lee, Satoshi Okabe, Jordan Peccia, Brent Peyton, Paul Sturman, Paul Stoodley, Rohini Srinivasan, Barbara Vaughn, Richard Veeh, Ernie Visser, and Mary Williams for their much appreciated assistance, laboratory techniques, and late night conversation. A special note of gratitude goes to Anne Camper for microbiological knowledge unavailable from anywhere else and Marty Hamilton and Kirk Johnson for their work with statistics. I am especially indebted to Richard Creed for emphasizing the value of fly fishing to my graduate studies.

Lastly, I would like to thank my parents, Ronald and Clarice Lundman, for their unending love and support throughout my longer-than-expected academic career.

TABLE OF CONTENTS

TABLE OF CONTENTS - Continued

LIST OF TABLES

LIST OF TABLES - Continued

LIST OF FIGURES

ABSTRACT

Packed bed or porous media type systems are a unique environment for bacterial growth. The large surface areas, plug flow mixing, and laminar hydrodynamics may offer the attached organisms higher nutrient concentrations at lower shear stresses when compared to regimes such as plug, laminar, or completely mixed flows. Industries affected by biological accumulations in porous media range from oil recovery to waste water treatment. Perspective may be the only factor in deciding whether such an accumulation is useful or detrimental.

As industry has become more aware of the importance of such accumulations, more emphasis has been placed upon modelling the affected systems. Two areas where modelling has suffered from a lack of data are cellular detachment rates and substrate transport. The objectives of this research were 1) correlation of cellular detachment rate with glucose utilization rate and 2) observation of changes in transport of dissolved components through the porous media as a result of the biological accumulation.

To accomplish these objectives, two series of experiments were run. A differential reactor was packed with 1-mm glass beads, inoculated with Pseudomonas aeruginosa, and operated at a constant flow rate. In the first series of experiments the inlet glucose concentration was 18 g m^{-3}. In the second series of experiments the glucose concentration was lowered to 2 g m^{-3}. This change in influent glucose concentration provided for a wide range of accumulation rates and glucose utilization rates. Cell concentrations and glucose concentrations were measured daily at the influent and effluent of the reactor. Stimulus-response studies were also performed daily.

Results indicated detachment rate was a function of glucose utilization rate. Theory suggested the correlation may be linear; however, noise in the data made this determination impossible. The stimulus-response studies demonstrated the strong dependence of mixing characteristics upon the extent of the biological accumulation.

INTRODUCTION

Industrial and Academic Relevance

Packed bed or porous media types of systems are a coupling of large surface areas, near plug flow mixing, and laminar flow hydrodynamics. These unique physical characteristics may offer attached organisms considerable advantages in the form of higher nutrient availabilities and lower hydraulic shear stresses when compared to true plug flow, laminar, or completely mixed systems. As a result of its existence, the biological accumulation alters both the chemical concentrations and flow regimes within the medium. The extent of profit or injury caused by the organisms is, as always, a matter of perspective. One thing is certain, biological accumulations in porous media or packed bed systems affect many industries.

The oil industry must respond to both the good and bad effects of these accumulations. Under the correct conditions, bacteria in oil formations (whether indigenous or introduced with the injection water) produce hydrogen sulfide, a process termed "souring". Souring decreases product quality and increases refining costs due to the complex handling procedures required for the toxic and strongly acidic hydrogen sulfide. To compound this problem, the bacteria may plug the formation (or the injection wells) once again raising recovery costs (McKinley, Costerton, and White, 1988).

Current research hopes to exploit this plugging phenomena. Bacteria injected into oil bearing formations may preferentially plug high permeability zones. This would enable waterflooding to liberate the oil trapped in zones of originally low permeability (Raiders,

Knapp, and McInerney, 1989). In addition, once in the formation, the bacteria may manufacture beneficial chemicals. The function of these chemicals could include dissolving of mineral deposits, acting as a surfactant, or altering fluid viscosities (Updegraff, 1990).

The ability of bacteria to degrade chemicals has long been known. Two industries making use of this knowledge are waste water treatment and bioremediation. Waste water treatment plants frequently employ trickling filters (downflow packed beds) to reduce chemical contents in municipal and industrial waste water to acceptable levels (Bryers and Characklis, 1990). Technology is currently being developed for both in situ (porous media) (Gannon, Manilal, and Alexander, 1991) and pump and treat (packed bed) bioremediation applications (Strandberg, Donaldson, and Farr, 1989).

Biological packed beds are also used for commercial chemical production. For example, E. coli immobilized in K-carrageenan beads are being used for the conversion of ammonium fumarate to L-aspartic acid (Hamer and Richenberg, 1988).

With the increasing interest in porous media and packed bed systems also comes an increasing value of predicting the extent and rate of associated biological processes. The modelling of these processes has been hindered by problems common to modelling biological accumulations in other geometries, 1) a poor understanding of the biological processes and 2) a poor understanding of the effect of the biological accumulation on hydrodynamics.

While the results of modelling are very sensitive to the process of biomass detachment, most times it is not directly measured. Modellers must use other measured variables to back calculate detachment rates. Thus, the accumulation must be largely described before it can be modelled and the utility of the model is diminished.

Substrate transport has suffered a similar fate. Due to the difficulty in determining mixing properties, most models assume completely mixed, laminar, or plug flow hydrodynamics. The effect of the biomass on hydrodynamics, and vice versa, is neglected.

Goal

The goal of this research was to quantify the effect of a biological accumulation on particulate transport and liquid mixing in a packed bed reactor.

Objectives

To accomplish this goal, the research was divided into two objectives. The first objective was to determine cellular detachment rate as a function of glucose utilization rate. The second objective was to determine the liquid mixing characteristics of the system and observe any changes in mixing as a result of the accumulating biomass.

Two series of monoculture, aerobic, packed bed experiments were run. For the first series, a high concentration of glucose in the reactor feed ensured that bacterial growth was limited by the concentration of dissolved oxygen. For the second series, a low concentration of glucose in the reactor feed guaranteed a glucose-limited system. The two extremes of growth provided for a wide range of mixing conditions and glucose utilization rates.

BACKGROUND

Transport Phenomena

The accumulation of biomass in any system is a complex product of two dependent phenomena, mass and momentum transfer. Whether the component of interest is particulate or dissolved, the system geometry significantly impacts the transport processes. Transport properties in porous media systems may deviate substantially from those seen in simpler geometries such as flat plates, closed conduits, or continuous flow stirred tank reactors (CFSTRs).

Particulate mass transfer in a porous medium may be described with the same general processes observed in other systems, with one addition, filtration. While filtration is theoretically possible in any system, it is usually negligible in systems other than porous media when compared to other transport mechanisms. Particle capture through size exclusion is an important feature of a porous medium. Variations in pore diameter may make it possible for a particulate of any size to be filtered. The effects are additive. As particles are filtered, more of the pore space is occupied by solids. Porosity is reduced, the average diameter of the pore spaces is decreased, and the rate of filtration is thereby increased.

Biomass may accelerate the filtration process quicker than abiotic particulates. As biomass is not a true solid, fluid may flow through the accumulated bacteria and extracellular polymeric substances (EPS). This is certainly true if the accumulation spans

the entire pore space. Any particle the same size as or larger than a bacteria could be captured.

Data from Rittmann and Wirtel (1991) and Sprouse and Rittmann (1990) suggest the capture efficiency of the media increases with increasing biomass regardless of mechanical filtration. Experiments conducted in a fluidized bed show that particle capture rates increased after the establishment of a biofilm. The biofilm therefore must demonstrate some degree of "stickiness" as size exclusion is nearly impossible in a fluidized bed.

The mass transfer of the dissolved components is also more complex in porous media. The path traveled by the fluid is highly variable in tortuosity, length, and diameter. This leads to a condition of enhanced longitudinal mixing when compared to closed conduit systems, a phenomena termed dispersivity.

Freeze and Cherry (1979) report dispersivity to be a function of three mechanical conditions resulting from the porous media geometry. First, mixing may be due to velocity distributions within a specific channel. Second, mixing may be due to variations in the pore velocities between channels of different size and roughness. Lastly, mixing may be due to the combining and splitting of channels. All three conditions contribute to a concentration profile within the system that may deviate significantly from what would be observed in a plug flow system.

The effect of a biological accumulation on these types of mixing characteristics is yet unknown. However, it may be expected that the intrusion of any particles into the pore spaces will distort the original fluid flow patterns, and thus biomass is expected to affect the mass transfer.

Conceptual Models of Biomass Accumulation

Two models are currently proposed to qualitatively describe the structure of cells and EPS within porous media. According to the first model, the biological accumulation is presumed to be a homogeneous mesh of polymer and cells completely filling the pores. Fluid in the reactor flows evenly throughout any given cross-sectional area. This model is unique in that it rejects the traditional view of fixed biological accumulations as necessarily being a film. No bulk fluid-biofilm interface exists. The true three dimensional nature of the media, bacteria, and bacterial products is highlighted.

The second model encompasses the more conventional model of biofilms. The reactor media may be visualized as numerous, parallel conduits with biofilm accumulations on the wall. Some points in a cross section may contain a very dense biofilm while others contain no biofilm. In this case, the biofilm may actually smooth and straighten the flow path. This model embodies the traditional bulk fluid-biofilm interface.

Taylor and Jaffe (1990) discuss both of these models in the first paper of their four-part series. They have named the two views the "closed" and "open" pore models, respectively. Results from their experiments indicate that flow through a porous media follows the "open" pore space model. Data from permeability reductions and dispersivity changes are used to support their conclusion.

Detachment Rates

Taylor and Jaffe (1990) performed mixed culture experiments in two identical, parallel columns packed with sand. The systems were then modelled. Data from the first

column was used to calibrate the model and data from the second was used to validate the calibration.

Detachment rates were incorporated into the model as a complex function that included terms to account for both the biological state of the organisms as well as the effects of physical shearing. No detachment rates were measured experimentally. Values were calculated from other measured variables.

The model indicated that significant errors occurred when detachment rates (shearing rates) were ignored. This was especially true for their system. It was demonstrated that the length of the column allowed the detached biomass to be filtered or reattach downstream. They noted the distribution of the biofilm on the particles largely influenced the detachment and reattachment of biomass. This influence was attributed to a nonuniform pore size distribution and thus nonuniform hydraulic environment.

Howell and Atkinson (1976) modelled trickling filters for use in the waste water industry. The model was unique for the time as it included sloughing. Their attention was drawn to the sloughing phenomenon after noticing that published data showed a high degree of variability. The efficiency of the filters, mass of biofilm in the filter, and biofilm thickness on the support particles cycled with time.

Their trickling filter model built upon a traditional tanks-in-series approach. Howell and Atkinson realized that while large parts of the film would slough, the entire accumulation would not slough simultaneously. To mimic this phenomenon, the tanks-in-series model incorporated a cyclic but random sloughing factor that affected only a small number of tanks at any one time. The results of this study came much closer than previous models to predicting the unsteady behavior of actual trickling filters. The overall conclusion was that the average values routinely employed in the design of trickling filters

were inadequate. Consideration of sloughing was essential as sloughing induced channeling and dead zones which significantly impacted the bed efficiency.

Rittmann (1982) proposed a steady state detachment rate model based entirely on the mechanics of shear stress. The model was born from criticism of a previous modelling effort by Rittmann and McCarty (1980), in which no account was given for biomass loss due to mechanical processes. In his treatise, Rittmann used a first-order model with parameters calculated using the data of Trulear and Characklis (1982) obtained in rotating annular biological reactors (RABRs). The model was extrapolated from the geometry of a rotating annulus to that of both packed and fluidized beds. As was expected, results indicated that shear losses were of increasing importance as shear stresses increased.

Rittmann also noted that use of a model with a first-order detachment rate coefficient gave numerical results similar to those given by existing models incorporating first-order endogenous decay coefficients as the two models were of essentially the same form. This numerical similarity was especially true at low shear stresses where the endogenous decay coefficient and the detachment rate coefficient could not be statistically differentiated.

Speitel and DiGiano (1987) noted that while detachment rates were definitely dependant upon shear stresses, higher detachment rates occurred during periods of high growth or high biodegradation. They experimentally determined rates of biomass loss in beds packed with granular activated carbon. The reactors were liquid-saturated and fed with either phenol or paranitrophenol. The inoculum was an undefined microbial population. The system was modelled building upon the work of Rittmann (1982). The detachment equation not only included a first-order term for shear loss due to mechanical

processes, but also included a Monod-type component which accounted for growth-based biomass loss. Results of the modelling effort agreed quantitatively with the experimental work. Comparison of the first-order equation of Rittmann to the data of Speitel and DiGiano showed very poor correlation at transient conditions. Higher than needed estimates of detachment at steady state, although qualitatively correct, were also noted.

The conclusion was once again that biomass loss was extremely important to the modelling process. In the model, biomass loss due to growth-based detachment accounted for 33% and 67% of new biomass formed, depending on the substrate. Based on this, Speitel and DiGiano concluded the parameters in the detachment rate equation, and thus detachment rates, were highly substrate specific.

Chang and Rittmann (1988) studied the effects of surface irregularities on detachment rates in packed columns. Two types of media, spherical and irregular granular activated carbon, were tested. Reactor design made independent measurement of important system parameters such as detachment rates impossible. A model previously developed by Chang and Rittmann (1987) calculated detachment rates using the first-order equation of Rittmann (1982).

For both reactor runs, Chang and Rittmann observed qualitatively the same detachment phenomena following biofilm establishment. However, at times early in the biofilm development, the irregular surface provided the attached cells better protection against shear stresses. The detachment rates were lower from the irregular surface when compared to detachment rates from the smooth surface. As the accumulations approached steady state, however, the detachment rates became very comparable. In fact, the detachment rates for both systems approached those predicted for smooth

surfaces. A step function best modelled the transition in detachment rates at early times to detachment rates at steady-state. Data within the time frame of high biomass accumulation (the transition phase) rates was neglected.

In a later study Chang, Rittmann, Amar, Heim, Ehliger, and Lesty (1991) studied the effects of abrasion on biomass loss. As the original intent was to demonstrate the advantages of fluidized beds over packed beds concerning plugging and channeling, a liquid-fluidized bed utilizing glass beads as support material was chosen for the study. Once again, a model was used to calculate variables that were not directly measurable. Results indicated that as the concentration of the glass beads in the reactor was increased, the detachment rate increased due to increased abrasion. However, the results were somewhat confounded by a simultaneous decrease in biofilm thickness and an increase in biofilm density, both of which partially offset the effects of increased abrasion. Most importantly, detachment rates in these systems were higher than those expected in non-fluidized systems. Abrasion was attributed to be the controlling factor in loss of bacteria from fluidized particles.

Peyton (1992) studied the effects of shear stress and glucose utilization rate on cellular detachment rates of Pseudomonas aeruginosa in RABRs. Results showed that over the narrow range of shear stresses studied, shear stress did not significantly affect detachment rate. Detachment rate was concluded to be most strongly correlated to the growth rate of the film. Therefore, a model was proposed which incorporated the variables influencing growth rate. Variables included in the proposed equation were yield, biofilm thickness, and substrate utilization rate. Detachment rates calculated from this equation gave significantly better results than those of Rittmann, Chang and Rittmann, Speitel and DiGiano, and others.

Stimulus-Response Experiments

Ever since Danckwerts' (1953) solidification of residence time distribution theory from vague concepts into a practical technology, the residence time study has received widespread application in flow systems as a tool for determining flow characteristics. In fact (and by his own admission), Danckwerts' original journal article has reached the stature of "a primary reference which is seldom cited" (Danckwerts, 1981). It shall remain so here.

Regardless of the lack of citations from his original article, Danckwerts did unite several ideas to form the foundation of a technology which is currently considered standard practice. The residence time of a tracer in a system or part of a system can be measured by introducing the tracer at the influent (the stimulus) and recording the concentration of the tracer as a function of time at the effluent (the response). Three methods of tracer injection have been effectively used as stimuli; step, pulse, and cyclic. All three methods can yield equivalent information, but the step and pulse methods are the more common. While cyclic tracer injections are theoretically equal to pulse and step injections, the mathematics and qualitative interpretation of the responses are considerably more complex.

If the pulse or step method of tracer injection is employed, the concentration of tracer at the influent as a function of time is usually assumed to form a "perfect" pulse or step respectively. For a pulse injection, this implies the influent concentration profile is a Dirac delta function. Often, if the time taken to introduce the tracer is very short compared to the residence time of the system, the injection is assumed to be perfect. For the step function, "perfection" implies the concentration of the tracer at the influent

is originally a constant and instantaneously changes to its final value. Step functions are also approximated as perfect if the time taken to complete the step is short when compared with the residence time.

A difference should be noted between the hydraulic residence time and the tracer residence time. Hydraulic residence time is the time the fluid spends in the system. This may not be equal to the time the tracer spends in the system. The residence time of the tracer will always be measured using the stimulus-response method. It then becomes a question of how well the tracer resembles the fluid or particulate for which the residence time is desired. The choice of the tracer is an important consideration in interpreting results. A pertinent example of this would be a system in which the tracer is absorbed.

Naor and Shinnar (1963) reiterate this theme by stating that if the tracer does not adequately represent the fluid of interest, the results will represent a response function to a change in concentration. They also explain that this may not be totally undesirable as it may provide important information, but the effect on the results should be noted. Difficulty in choosing an adequate tracer may be the main reason residence time studies have not received more use in studies of biological systems.

Naor and Shinnar also point out that the response of the system to the stimulus must be linear if the step and pulse inputs are expected to yield identical information. A linear response is always received if the tracer is nearly ideal; however, if a less-than-ideal tracer is employed, a non-linear response must also be noted. Swaine and Daugulis (1988) cover, among many other relevant topics, the process of tracer selection in some detail.

For systems in which residence times are short, the time needed to inject the tracer may be significant when compared to the mean residence time. The pulse can no

longer be considered as a perfect Dirac delta function, but it is still possible to calculate a residence time by measuring the concentration of the tracer as a function of time at both the inlet and outlet of the reactor. This technique has been named the imperfect pulse method.

The main disadvantage to the imperfect pulse method lies in tailing. Tailing occurs when the concentration of tracer at the point of measurement maintains a low, but non-zero, value for an extended period of time. Any tailing in the inlet signal will cause an even larger tailing effect in the outlet signal.

If the traditional analysis of moments is performed, tailing will severely skew the results. The region where the measurements are generally least accurate is the region of lowest tracer concentration, the tail. This is also the region where the largest time values occur. The mathematical equation used to calculate residence times is strongly influenced by large time values if the concentration of the tracer is not zero. Large time values translate into long residence times if tailing is present.

Advanced mathematical techniques such as Laplace transforms (Ostergaard and Michelsen, 1969) or Fourier transforms (Condoret, Riba, and Angelino, 1989) must be used to improve the accuracy of the calculations. Anderssen and White (1971) state that even the use of these methods is not foolproof as the choice of the weighting parameters for such techniques will influence the results. Not surprisingly, optimization of the weighting parameters may be more than trivial.

Tracer studies have been applied to a myriad of abiotic systems; however, the application of the same technology to biological systems has been lacking. Without doubt, the presence of a biological component complicates the implementation of the experiment and the interpretation of the results. This lack of application has been

especially tragic considering the large effect such a biological accumulation may have on the flow regime. Most published material involving tracer studies in biological systems concern three large industrial applications; waste water treatment, immobilized enzyme catalysis, and fermentation.

Kennedy and Droste (1985) described the factors affecting the startup of anaerobic downflow trickling filters for treatment of waste water. As part of the research, stimulus-response studies were performed on the reactors after establishment of a mature biofilm. A pulse of tritium was injected into the recirculation line and aloquots of effluent were taken at short intervals for approximately 3 hydraulic residence times. The experiment was replicated for three different feed flow rates (varying by a factor of 17). The recovery of tracer was reported to have been in excess of 90% for all cases. The results of this study indicated the flow regime in the reactor was that of a CFSTR. The CFSTR type behavior was attributed to biogas production. They proposed the biogas may have acted as a gas lift pump causing a large degree back mixing.

Suschka (1985) reviewed previously published residence time studies on biological percolating filters. Experimentally measured residence times were found to be at least three times longer than those predicted from falling-film theory. To explain this large disparity, a reactor model was devised in which two distinct liquid layers existed. The first liquid layer was free flowing over the surfaces. The second was captured within the biofilm. Under this scheme, the liquid volume maintained in the reactor would be much larger than values calculated from the older flat-plate, falling-film model.

This two-layer model was used to explain high effluent oxygen concentrations in a seemingly anaerobic reactor. The free flowing layer could have maintained high oxygen

concentrations because the diffusion of oxygen into the film was slow when compared to the residence time of the liquid in this layer.

Guzy, Saidel, and Lotan (1990) applied a tanks-in-series model to an immobilized enzyme packed bed reactor fed with two differing substrates. Tyroglubin, a high molecular weight (669,000 Daltons) protein was pulsed into the reactor. The high molecular weight minimized liquid diffusional effects and eliminated diffusion of the tracer into the pores of the packing. The concentration of tracer in the effluent was monitored continuously via absorbance measurements.

The number of tanks-in-series needed for modelling a particular flow rate was calculated from the residence times and variances of the response curves. The residence time curves indicated that the number of tanks required to model the range of flow rates was not a monotomic function of the flow rate, but was the result of two competing processes, mechanical agitation and diffusion.

The problems associated with the perfect pulse injection method were seen in this study. At the highest flow rate, the residence time was approximately 12 seconds while the tracer injection time was 2 seconds, not a negligible difference. Thus, the results may have been confounded by a poor method of analysis. No effort was made to deal with the imperfect stimulus.

Anselme and Tedder (1987) reported tracer studies for determination of the flow regime in a packed bed bioreactor. Yeast cells were immobilized and fed glucose to produce ethanol. Of the various types of support media investigated, crushed brick provided the best performance and was therefore used in most of the experiments, including the residence time determinations. A step change in ethanol concentration was introduced at the inlet of the column. The effluent was collected and ethanol

concentrations determined with a gas chromatograph. Results indicated that axial dispersion was important to modelling the flow. It was also noted that improved culture stabilization techniques were needed to prevent plugging of the pores from cell debris.

Similarly, Godia, Casas, and Sola (1987) reported on the fermentation of glucose to ethanol in a bioreactor packed with yeast immobilized in carrageenan gel beads. A tracer study was conducted via a step introduction of lactose at the column inlet. Results showed the packed column had flow characteristics best represented by a tanks-in-series model. This CFSTR behavior was once again attributed to a large evolution of carbon dioxide with the degree of backmixing too large to be modelled by dispersion alone.

Gonzalez, Caminal, de Mas, and Lopez-Satin (1989) operated a column packed with ground wheat straw which was enzymatically hydrolyzed to sugar. To study the bed hydrodynamics a step perturbation of potassium chloride was introduced at the inlet. The conductivity of the reactor fluid was then measured near the outlet. Axial dispersion in the reactor was found to be negligible. The reactor was subsequently modelled as plug flow. Porosity of the system was calculated from the measured response curves. The liquid volume of the reactor was computed as the flow rate divided by the residence time. Liquid volume then divided by the total reactor volume yielded the porosity.

Hamamci and Ryu (1987) investigated the use of a tapered bioreactor filled with yeast immobilized in carrageenan to produce ethanol from glucose. A tapered column was chosen to alleviate the mixing problems associated with the evolution of large quantities of carbon dioxide. The dispersion parameters for the hydrodynamic model, however, were determined in a cylindrical column. This allowed the authors to calculate the dispersion parameters from the already well established equations for flow through a round conduit. The tracer was blue dextran. Once again this tracer was chosen

because of its high molecular weight which reduced diffusional problems. The concentration of the blue dextran at the effluent was determined via a spectrophotometer. Over the range of flow rates employed in the study, it was determined that the dispersion was significant, but relatively constant.

MATERIALS AND METHODS

Laboratory Techniques

Experimental Design

Two modes of operation, constant flow rate and constant pressure drop, are commonly seen in liquid-saturated porous media systems. However, setting often dictates the frequency of occurrence. In natural environments, constant pressure systems are prevalent. Obvious examples include aquifers and oil reservoirs. In man-made locations, constant flow systems such as packed columns are predominant.

For reasons related to laboratory operation, this project employed a constant flow system. From preliminary work, it was concluded that constant pressure drop systems suffered from catastrophic plugging problems associated with the biological accumulation. The extremely low flow velocities, resulting from the plugged media, created significant contamination and sampling problems. A constant flow rate system was chosen because of the ability to maintain higher flow velocities.

As the results from this research were to be applicable to other projects, Pseudomonas aeruginosa, an aerobic, Gram negative, bacteria was chosen for study. The bacteria had already received considerable attention from the research community and as a result was better characterized than most species. It was hoped that information from these experiments could be added to a large data base already receiving use in predictive modelling. Following this same theme, the substrate chosen was glucose (the

substrate for which the most information regarding growth of Pseudomonas aeruginosa was available).

In order to test extremes of bacterial growth, the experiments were divided into two series. In the first series the influent glucose concentrations were maintained at 18 g m^{-3}. This high concentration of glucose implied the bacteria would experience oxygen-limited growth as their oxygen requirements would exceed the solubility of oxygen in water at the operating temperature. Thus, the biological activity would be at a maximum for an aerobic system in which the oxygen was supplied by means of dissolved air. The second set of experiments were run with an influent glucose concentration of 2 g m^{-3}. This left the bacteria glucose limited and growth rates were lower.

The reactor was sampled approximately once per day. Samples were taken from the influent and effluent of the reactor for determination of glucose and cell concentrations in the bulk fluid. Pressure drop across the reactor was recorded. Stimulus-response curves were collected using the method of imperfect pulse tracer injection with a salt solution as the tracer. The concentration of salt was proportional to the conductivity of the liquid. The progress of the pulse through the system was measured by conductivity probes at the inlet and outlet of the reactor.

Three runs were made for the first series and two runs for the second series. At the end of one run from each series, an experiment was performed to determine the permeability of the reactor (including the accumulated biomass) to cells in the bulk fluid (microbead penetration experiments). At the end of the other runs, the reactor was disassembled and the quantity of biomass weighed. Not until after the first two runs of the first series were the microbead penetration experiments determined to be necessary.

Therefore, a third experiment was run for this series. No other measurements were taken from the third run except the microbead penetration data.

To determine the permeability of the system to bacteria, fluorescent latex microbeads (Polysciences, Inc., #15705) were injected as a pulse into the reactor. The fraction of beads leaving the reactor and distribution of beads captured in the reactor after 10 minutes were counted. After 10 minutes, the reactor was disassembled. Sections of the glass beads inside the reactor were distributed into beakers based upon distance from the inlet. The beakers, along with the reactor contents, were dried. To enable counting, the microbeads were resuspended with a known quantity of water and the beakers placed in an ultrasonic water bath for a minimum of 30 minutes. The ultrasound treatment insured the microbeads were completely removed from the surface of the glass beads.

It was assumed from physical similarities between the bacteria and the beads, that the performance of the beads while passing through the reactor imitated that of the bacteria. The beads were spherical with a 1 μm diameter, a specific gravity of 1.05, and a negative surface charge (Drury, 1992).

Reactor Design

To obtain meaningful data, a reactor in which the biofilm properties remained constant as a function of axial length was desired. Due to a lack of a better measurement, thickness was chosen as the characteristic on which the criteria of "constant" biofilm properties was applied. From previous efforts by Abedeen (1990) and

Crawford (1987), the maximum length over which the biofilm thickness could be expected to remain constant was 50 mm. Thus, 50 mm was chosen as the reactor length.

The final reactor design is shown in Figure 1. The reactor housing was cut from cylindrical glass tubing 31 mm in diameter. The diameter was chosen to yield a minimum bed diameter to particle diameter of 30. This was the smallest ratio recommended by Cohen and Metzner (1981) (for newtonian fluids) allowing wall effects on packing geometries and fluid flow to be neglected. The minimum ratio was exceeded as the packing was previously chosen to be 1-mm glass beads.

Brass gauze (#30) over each end of the reactor retained the beads in the bed. Flow was dispersed by funnels attached to each end of the reactor with silicon sealant. The influent funnel contained a stainless steel ball to further insure even distribution of the fluid. Pressure taps, liquid sampling ports, and conductivity probe ports were provided at each end of the reactor at the gauze-bead interface.

For the first run, the conductivity probes were cemented directly into the reactor. This resulted in poor data because the probes could not be calibrated. The reactor design was subsequently changed. For the remaining three runs a septum was built into each end of the reactor through which a conductivity probe was aseptically inserted and removed as needed for calibration.

Support Apparatus

The support systems for the reactor are shown in Figures 2 and 3. Dilution water was pumped to the reactor from a 0.125 m^3 aerated supply tank. This tank provided for a 2-day reserve of distilled water if the house water supply were interrupted. Particulates,

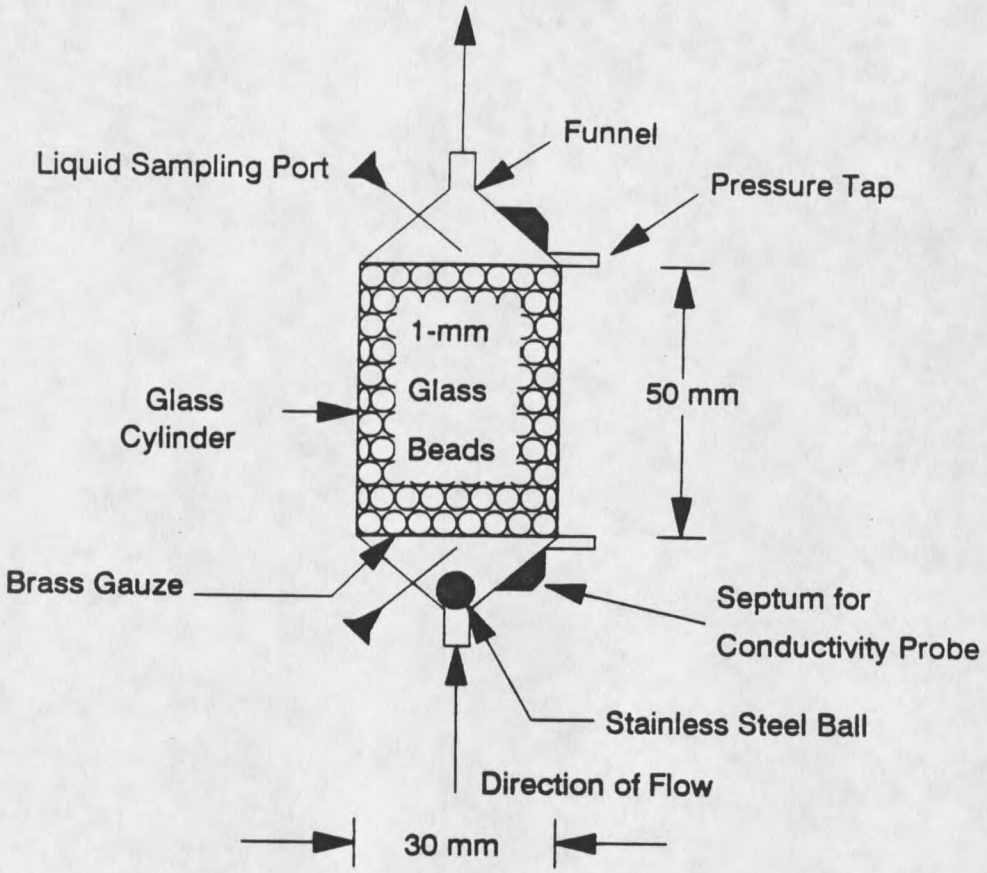

Figure 1. Detailed diagram of final packed bed reactor design.

including bacteria, were removed from the dilution water by two in-line 0.2 μm cartridge filters (sterile). After filtration, the sterile dilution water flowed through a 1.5 m stainless steel coil submerged in a constant temperature (20°C) water bath. Nutrients were added to the bulk liquid just prior to the reactor influent.

To prevent contamination, the minerals were divided into two carboys. The glucose and phosphates were isolated from the nitrates and other minerals in an attempt

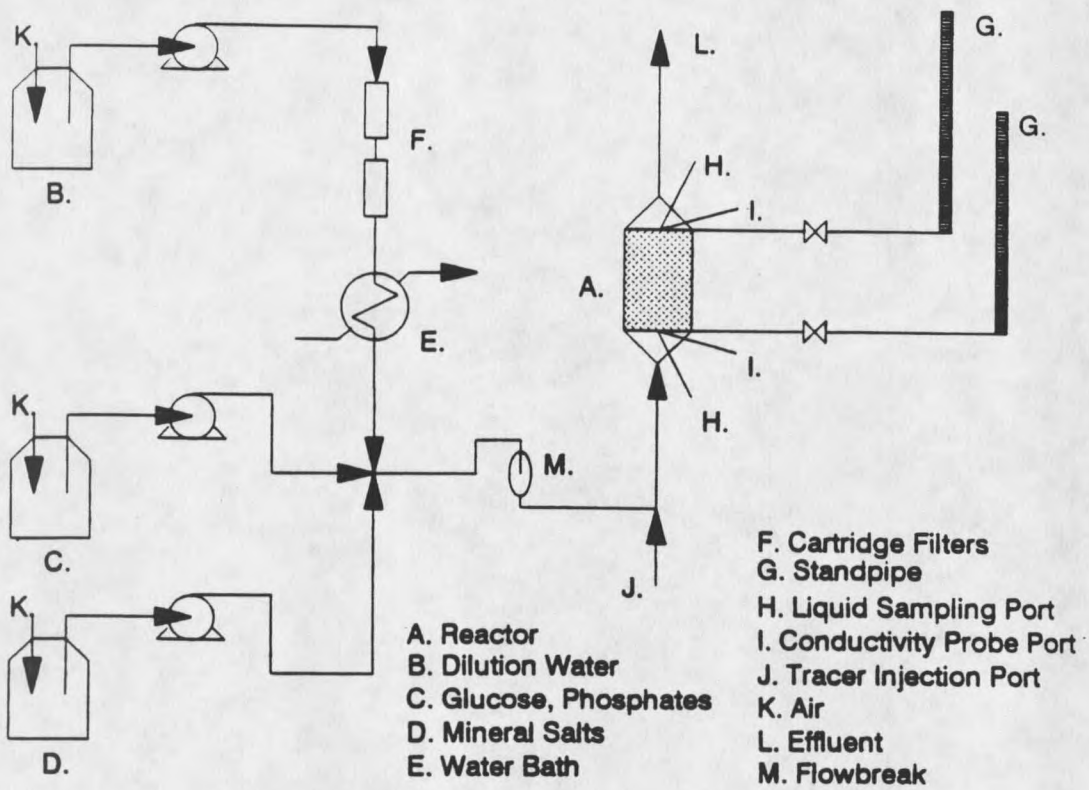

Figure 2. Schematic of apparatus used in high glucose loading rate experiments.

to produce a nutrient-limited environment in both containers. Should the bacteria contaminate either feed container, the extent of growth would be minimal.

The mineral salts and glucose were prepared to be 100 times the recommended concentration (Sieble 1987) and mixed with the dilution water in a ratio of 1 part feed to 99 parts water. A complete table of minerals and concentrations is given in the appendix. While the temperature of the minerals and substrate was not controlled, the effect on the

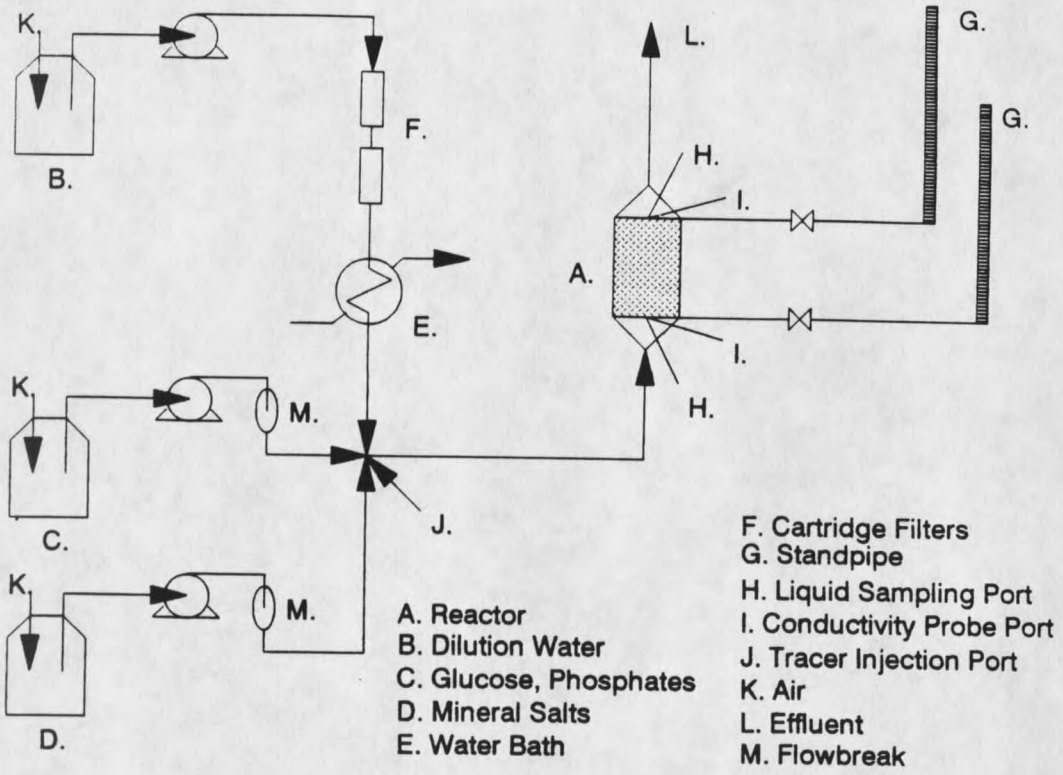

Figure 3. Schematic of apparatus used in low glucose loading rate experiments.

overall fluid temperature was negligible.

For the first series of experiments (see Figure 2), the nutrients were mixed with the dilution water before the flow break. The flow break was included to ensure that bacteria from the reactor did not migrate upstream into the nutrient reservoirs. An injection port for the salt tracer was located approximately 15 cm ahead of the reactor (down stream of the flow break) for the first series of experiments.

For the second series of experiments (see Figure 3), the tubing configuration was altered. Flow breaks were added to both feed lines and the flow break was removed from the dilution water line. The nutrient and tracer injection points were moved much closer to the reactor. This reduced cell concentrations at the reactor influent by eliminating a significant portion of the surface area (tubing wall) previously available for colonization.

All the tubing used in the experiment was Masterflex™ silicone (oxygen permeable) tubing. The pumps used were Masterflex™ peristaltic pumps (1-100 rpm).

Conductivity Measurement

The system for measuring liquid conductivities was originally used by McCready (1977) to determine the mixing characteristics of static mixers. Unfortunately, McCready's conductivity probes were much too large to use in this study. For this experiment, probe size was extremely important. First, the conductivity probes needed to be small enough to insert through a septum without causing leakage upon removal. Second, the probes needed to be small enough to not significantly disturb flow through the reactor.

As a solution, the probes (see Figure 4) were constructed from stainless steel syringe needles. The probe design was originally forwarded by Lamb, Manning, and Wilhelm (1960). However, the design was subsequently miniaturized by Larsen and Keck for work presented by Keck (1987).

Probe operation was based on the flow of electricity through a fluid separating two electrodes. One electrode acted as a current source, while the second received the fraction of the current which was able to pass through the liquid. Any change in liquid

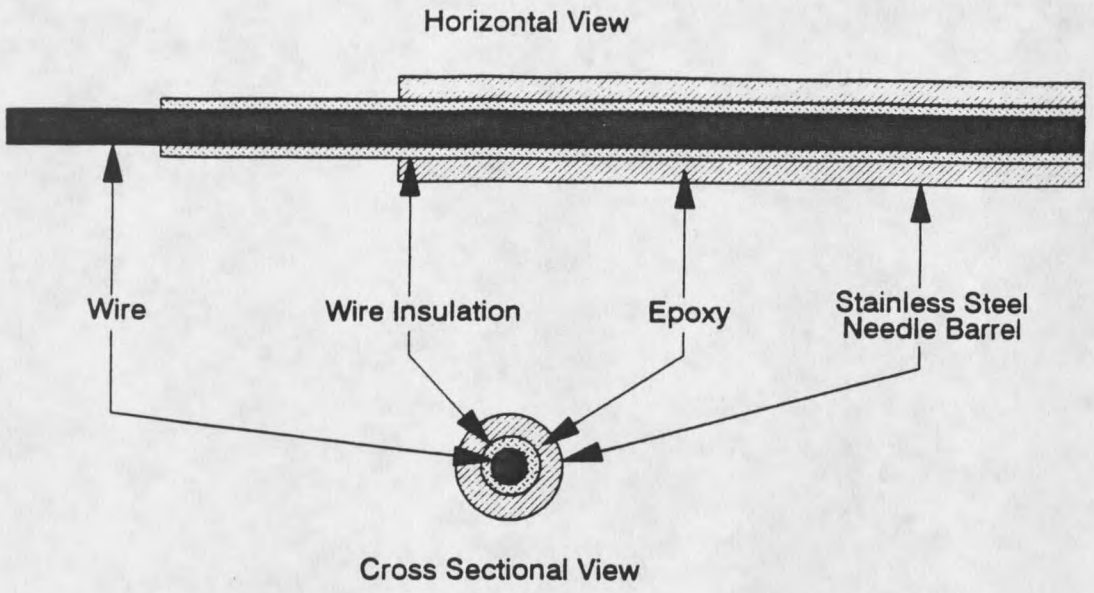

Figure 4. Detailed diagram of conductivity probe assembly.

conductivity would have resulted in a change in current passing through the probe.

Probe construction for this experiment was simple. An insulated wire was passed through a hypodermic needle and cemented with epoxy. The needle-wire assembly was cut off square at the sharp end of the needle. The end of the wire was thus exposed, but protected. One lead from a sine wave generator was connected to the wire in the center of the probe. The other lead (the ground) was connected to the needle. Therefore, the syringe needle was not only a protective housing, but also an integral part of the probe.

The probe was fed an AC signal of constant frequency (1460 Hz) and voltage (3V) from the wave generator. Attenuation of the signal at the probe tip was directly proportional to the conductivity (resistivity) of the liquid. The attenuated signal was then

amplified and rectified. The demodulated (DC) signal in the form of a voltage was read and stored by a computerized data acquisition system.

During the first run, the gain and offset of the DC signal were coupled within the amplifier (the higher the gain the larger the output voltage). This proved unsatisfactory. The attenuated signal required amplification to a degree to which the data acquisition system could no longer read the signal.

This problem was solved in two steps. First, an offset was added to the electronics after the demodulator so that the demodulated signal could be adjusted to any of a wide range of voltages. Second, a new data acquisition board capable of registering twice the voltage range as the original board was installed in the computer. As a bonus, the new data acquisition board allowed the gain to be increased even more (increasing the sensitivity of the readings).

System Operation

Prior to start up, the system was autoclaved intact at 18 psig and 125°C for 1 hour. The nutrient carboys were the one exception to this procedure. The carboys were separated from the system and autoclaved separately. The large liquid volumes required a minimum of 4 hours autoclaving to be properly sterilized. The remainder of the system could not withstand such a long time in the autoclave.

Once sterile, the reactor was inoculated with Pseudomonas aeruginosa. Prior to inoculation, the bacteria were grown aerobically in batch culture at 35°C for approximately 2 days, giving a final cell concentration of ca. 10^7 cells ml^{-1}. The culture media consisted

of the same mineral salts media used in the flow experiments. The initial glucose concentration for the batch cultures was 1000 mg l^{-1}.

The inoculation proceeded as follows. The reactor was isolated from the system by clamping the inlet and outlet tubing. Through the influent sampling port, the reactor was filled with the batch culture media. The system was then left, undisturbed, for a four-hour period. This allowed the bacteria to attach to the surfaces of the glass beads. After four hours, the hose clamps were removed. The reactor was subsequently operated in upflow mode at a constant flow rate of 38 ml min^{-1}.

Glucose and suspended cell concentrations at the influent and effluent were monitored, pressure drop across the reactor was measured, and stimulus-response studies were performed daily. Liquid samples for determining glucose and cell concentrations were drawn through the sampling ports into 60-ml sterile syringes. When attaching or detaching the syringes, the ports were flamed with ethanol and aseptic conditions were maintained.

For the first run of the first series, only one syringe volume was withdrawn per sample. This sample was analyzed only once. Due to variance in the data, the sampling design was modified.

For the second run in the first series, three separate reactor samples were taken and three subsamples of this reactor sample were analyzed in triplicate. This procedure gave extremely precise results; however, the time requirements were prohibitive. Statistical analysis revealed the main source of sample variation to be from reactor sampling error (Johnson, Lundman, and Hamilton, 1992). The sampling schemes for the two remaining runs were again redesigned.

For the remaining two runs, three syringe volumes were withdrawn from the reactor. The three samples were homogenized and one sample was analyzed from the composite.

All samples were preserved immediately after withdrawal. Cell samples were preserved in a buffered formalin solution (Griebe, 1991). Glucose samples were centrifuged (to remove cells and EPS) and frozen.

Each experiment ran for two weeks or until a system failure forced shut-down. An exception to this was the microbead experiment conducted at the high glucose loading rate. This experiment was run for only one week.

Analytical Techniques

Cell Concentrations. Suspended cells were counted using epiflourescent enumeration. A known quantity of a preserved cell sample was stained and filtered onto a black, 0.2μm polycarbonate membrane. The cells on the filter were enumerated under ultraviolet light (UV).

Cells taken from the reactor during the first run of the first series were stained with Hoechst 33342 or 6-Diamidino-2-phenylindol (DAPI). Use of the Hoechst stain was subsequently discontinued due to rapid loss of fluorescence during exposure to UV light.

All cell samples from the remaining three runs were double stained with DAPI and Acridine orange as described by Griebe (1991). Double staining allowed for easier distinguishing of cells from EPS. The DAPI stained only the cells, while the Acridine orange stained both EPS and cells.

In the first run of the first series, a computer processed the microscope image as seen through a video camera. Once calibrated to record only objects of similar size and color to bacteria, the computer counted the number of such objects in the field. The procedure was repeated until approximately ten fields or 300 cells had been imaged. By knowing the area of the viewing field, the area of the filter paper, and the amount of sample filtered, a concentration of cells in the original sample could be calculated. Due to the slowness of the imaging process, this method was abandoned as unfeasible.

For the last three experimental runs, the image analyzing system was excluded from the counting process. Instead, an etched grid was inserted into the ocular of the microscope, and the number of cells per field was counted manually. The surface area of the grid was calibrated against total magnification. This resulted in a much faster procedure with no loss of accuracy.

The number of fields counted varied significantly between runs. For the first run of the first series, 10 fields or 300 cells were counted for each slide. For the second run in the first series, only 10 fields per slide were counted, allowing the data base for the statistical analysis to contain a constant number of field counts per slide (a convenience for data handling).

As statistical analysis subsequently showed, ten field counts per slide were inadequate. For the remaining two runs in the second series, the number of fields counted was increased to 20 per slide.

Microbead Concentrations. The microbead concentrations were determined using techniques similar to those of cell enumeration. However, no staining was necessary as the microbeads were manufactured to fluoresce under UV light.

Glucose Concentrations. Glucose concentrations were determined colorimetrically using Sigma Diagnostics® enzymatic glucose determination (procedure no. 510). This procedure employed two enzymatic reactions. In the first reaction, glucose oxidase converted the glucose present into gluconic acid. In the second reaction, peroxidase reacted with the gluconic acid produced in the first reaction to produce ortho-dianisidine. The ortho-dianisidine was brown in color and could thus be detected via absorbance spectrophotometry. Over a wide range of glucose concentrations the absorbance of the ortho-dianisidine correlated linearly. As the enzymatic kit was originally designed for much higher glucose concentrations than those used in these experiments, the concentrations of the reactants were modified to correspond to the range of expected glucose readings (Peyton 1992).

Glucose samples were subjected to the same statistical analysis as the cell samples. For the first run in the first series, a single glucose sample was taken from the reactor and analyzed in triplicate. The second run of the first series required triplicate reactor samples be analyzed in triplicate. Data from the second run provided the statistical basis for modifying the sampling and analysis techniques in the remaining two runs in the second series. For these runs, a composite sample was analyzed in duplicate.

Pressure Drop. Pressure drop across the reactor was measured using two vertical stand pipes, one at the entrance and one at the exit. The pressure drop across the reactor was recorded as the difference of the height of the water between the tubes. This was the true dynamic pressure drop. Due to surface tension between the beads and water, the stand pipes indicated no static head in the reactor.

Stimulus-Response Studies. As the final measurement, a stimulus-response study was conducted. Conductivity probes were placed at the influent and effluent of the reactor. For the first run of the first series, a small quantity of saturated sodium chloride solution (filter sterilized) was injected at the port directly upstream of the reactor. As the salt passed the probes, an increase in conductivity of the solution, due to the higher concentration of salt ions, was recorded by a computer data acquisition system as an increase in a voltage signal. A minimum of three break-through curves were recorded per day.

This procedure was modified after the first run of the first series. The sodium chloride solution was replaced with a solution of mineral salts identical to the concentrated mineral salts fed to the reactor. The mineral salts were concentrated 100 times as compared to background levels. This change of salt solutions reduced detrimental effects the tracer may have had on the bacteria.

As mentioned earlier, the probes were made removable to allow each probe to be calibrated. The probes were flamed with ethanol prior to insertion through the septa.

After three stimulus-response curves were recorded, the probes were calibrated. From the influent and effluent of the reactor, 50 ml of fluid were removed and placed in separate stirred beakers. The probes were removed from the reactor and the tips submerged in the solution of the respective beaker. Known volumes of the concentrated mineral salts were simultaneously added to both beakers and the voltages from the probes recorded.

Biomass Quantification. The mass of biological material in the system was determined by weighing. The contents of the reactor were emptied into a "precooked"

dish. The dish had been heated in a muffle furnace (525°C) for a minimum of four hours. This "cooking" process removed all volatile compounds from the dish. The dish containing the reactor contents was placed in a 100°C drying oven overnight. The container and biomass were then weighed. To remove the volatile biomass, the container and biofilm were again cooked for four hours in the muffle furnace. After cooking, the dish and contents were reweighed. The difference between the weight before and after cooking was recorded as the mass of volatile solids.

Data Analysis

Detachment Rates

If the reactor used in the study were truly differential, the mass balance equations would have the same form as those of a CFSTR. A mass balance on cells suspended in the bulk fluid would yield the following equation.

$$V \frac{dX}{dt} = Q (X_i - X_e) + \mu X_e V + R_d A - R_a A \qquad (1)$$

Assuming the residence time to be very small allows the effect of growth to be neglected ($\mu X_e V=0$). Also, because the rate of attachment is assumed very small when compared to detachment, $R_a=0$. This allows the equation to be simplified to the following.

$$V \frac{dX}{dt} = Q (X_i - X_e) + R_d A \qquad (2)$$

One further simplification allows for the calculation of detachment rates from a minimum of experimental data.

If the left side of the equation is very small when compared to the terms on the right (pseudo-steady state) then the following equation is true upon rearrangement.

$$R_d = \frac{Q}{A} (X_e - X_i) \qquad (3)$$

This, in fact, is possible to demonstrate for both true steady state and transient conditions.

At steady state the accumulation term is by definition zero. In the transient state the accumulation term is not exactly zero, but the time scale for accumulation is very large when compared the time scale for detachment. The terms on the left side of equation (1) can be demonstrated to be many orders of magnitude less than those on the right.

Detachment rates were thus calculated from Equation (3). The flow rate used in the equation was the average for the experiment. The area used in the calculation was that of the clean reactor (glass beads and walls).

Substrate utilization rates for correlation with detachment rates were calculated from the following definition.

$$R_U = \frac{Q}{A} (S_i - S_e) \quad (4)$$

Pulse Tracer Studies

Analysis of Moments. The most common parameter calculated from the stimulus-response curves is the residence time of the signals. By methods of ordinary analysis, the residence time or first moment about the origin, $\bar{t}$, is:

$$\bar{t} = \int t \cdot E(t)\, dt \approx \sum_{j=1}^{n} t \cdot E(t_j) \cdot \Delta t_j \quad (5)$$

where:

$$E(t) = \frac{C(t)}{\int C(t)\, dt} \approx \frac{C(t_j)}{\sum_{j=1}^{n} C(t_j) \cdot \Delta t_j} \quad (6)$$

If the perfect pulse method is employed, this value is only calculated for the response curve and is deemed the mean residence time. By definition the stimulus has a residence time of zero. However, if the imperfect pulse method is used, the mean residence time of the system becomes the residence time of the response curve minus the residence time of the stimulus curve (equation (7)).

$$\tau = \bar{t}_{response} - \bar{t}_{stimulus} \quad (7)$$

Unfortunately, the ordinary analysis of moments may give poor results when tailing is present. The tail of the curve is the region of lowest tracer concentration and often the least accurate part of the curve. The tail is also the region that most affects the mathematics because of the large time values. A long tail which is an artifact of poor measurement accuracy can shift the moments significantly.

Weighted Moments. Imperfect pulse experiments suffer severely from tailing. The stimulus curve usually contains some degree of signal tailing which is propagated into the response curve. To alleviate the problems associated with tailing, the tail portion of the curves may be truncated by weighting.

An exponential term may be included in the moment integral. The resulting equations are the Laplace transforms for the functions. For determination of residence times, the equation becomes:

$$\bar{t} = \frac{\int t \cdot E(t) \cdot e^{-s \cdot t}\, dt}{\int E(t) \cdot e^{-s \cdot t} dt} \approx \frac{\sum_{j=1}^{n} t_j \cdot E(t_j) \cdot e^{-s \cdot t_j} \Delta t_j}{\sum_{j=1}^{n} E(t_j) \cdot e^{-s \cdot t_j} \Delta t_j} \qquad (8)$$

The weighting parameter, s, is theoretically arbitrary, but in practice may have a significant impact on the results. If too small, the tail will not be shortened enough to correct the original problem. (Note that if s=0 the equation returns to being the ordinary analysis of moments.) If s is too large, the curves will be prematurely truncated and the

results distorted. To choose a value of s that is close to its optimum value, Anderssen and White (1971) recommend the following equation.

$$s = \frac{2(k_{ave}+1)}{(\bar{t}_{stimulus}+\bar{t}_{response}-t_D)} \qquad (9)$$

The term t_D is the time delay between the stimulus and response signals or, basically, the breakthrough time of the response curve. If the beginning of the stimulus signal is considered to be time zero, t_D is the time of breakthrough for the response curve. It should also be noted that the residence times used in this equation are those of the ordinary analysis of moments.

The average order of the moment, k_{ave}, is defined as follows with k_{max} being the largest order of the moment used in the calculation. In this case k_{max} was 2 as variances were calculated but not included in the thesis.

$$k_{ave} = \frac{k_{max}}{2} \qquad (10)$$

For this experiment the mean residence times were calculated using the modified method of moments. It was necessary, however, to calculate the residence time of the curves using the ordinary analysis of moments so that the weighting factors could be generated.

As a criteria to determine the validity of the experimental curves, the areas of the stimulus and response curves were calculated and compared. For the curves to be valid, the areas needed to be equal. If more than one of the three sets of stimulus-response

curves were good (based on a comparison of the areas), the good curves were aligned then added. The point of alignment was chosen to be the initial rise of the stimulus curve. The addition of the curves provided an average of the data.

RESULTS AND DISCUSSION

Detachment Rates

Latex Microbeads

The latex microbead experiments demonstrated the ability of bacteria entering the reactor to penetrate the entire length even after large amounts of biomass were present. Of the total number of beads injected, 5% and 23% of the beads, for the experiments run with inlet glucose concentrations of 2 and 18 g m^{-3} respectively, were captured in the reactor.

This high degree of penetration was very important to the theory and calculation of the detachment rates. Influent cell concentrations were required measurements as a large fraction of the cells entering the reactor or detaching from any part of the reactor would be counted in the effluent. The reactor was therefore differential with respect to particles, and as such, the entire surface area of the reactor needed to be included in the detachment rate calculations.

Literature suggests that the quantity of particulates captured increases with increasing biomass quantities (Sprouse and Rittmann, 1987; Rittmann and Wirtel, 1991). The microbead experiments supported this conclusion. The percentage of beads captured by the reactor for the low glucose loading rate experiment was indeed lower than the percentage of beads captured by the reactor for the high glucose loading rate experiment. As will be discussed later, the reactor for the low glucose loading rate

experiment contained much less biomass than the reactor operated at the high glucose loading rate.

Table 1 shows the distribution of the latex beads remaining in the reactor as a function of axial position and glucose loading rate. No conclusion could be drawn as to the existence of a biomass gradient as a function of axial position. The concentration of beads in the reactor from the high glucose loading run decreased slightly from the inlet to the outlet whereas bead concentrations in the reactor used in the low glucose loading rate experiment increased from inlet to outlet. The differences in the influent and effluent concentrations did not appear to be outside of errors expected from this type of count data (Johnson, Lundman, and Hamilton, 1992). Therefore, the distribution of beads, and thus biomass, within both reactors was concluded to be nearly uniform. No attempt was made to weigh the mass of biological material in the reactor as a function of length.

Unfortunately, no direct comparison of bead numbers can be made between the two experiments as only one-fourth of the beads injected into the reactor for the high glucose loading rate experiment were injected into the reactor for the low glucose loading rate experiment. However, while the number of beads injected into the reactor for the high glucose loading rate experiment was only a factor of four larger than that injected into the reactor for the low glucose loading rate experiment, the reactor operated at the high glucose loading rate captured over thirty five times more beads than the reactor operated at low glucose loading rates. This again indicated that an increased amount of biomass increased capture.

As a final note, it should be mentioned that the small degree of bead capture and the nearly flat distribution of beads within the reactor were in some ways a fortuitous

property of the system. As filtration is a function of the ratio of pore to particle diameter, a smaller ratio would have increased filtration due to size exclusion. This system had a pore to particle diameter ratio of approximately 100 based on a clean reactor. Thus, it was assumed that the majority of bead capture was due to the presence of the biomass.

Table 1. Distribution of Latex Beads within Reactor

Distance from Inlet, x (m)	Bead Conc. ($x10^9$ beads m^{-1})
18 g m^{-3} glucose inlet concentration	
$0.00 < x \leq 0.01$	156
$0.01 < x \leq 0.02$	128
$0.02 < x \leq 0.03$	130
$0.03 < x \leq 0.04$	82.2
$0.04 < x \leq 0.05$	41.5
2 g m^{-3} glucose inlet concentration	
$0.000 < x \leq 0.014$	1.99
$0.014 < x \leq 0.025$	2.86
$0.025 < x \leq 0.031$	3.27
$0.031 < x \leq 0.05$	3.75

Process Rates

In order to calculate the substrate utilization and detachment rates, the flow rate of liquid through the reactor was needed. The target flow rate for each experiment was

approximately 38 ml min^{-1}. The average of the recorded flow rates were 38.3, 38.5, 38.5, and 38.6 ml min^{-1} for series one,run one; series one,run two; series two, run one; and series two, run two, respectively.

Substrate Utilization Rates. Specific glucose utilization rate as a function of time is shown in Figure 5. In all cases the specific glucose utilization rate increased from zero (no feed, no bacteria) at time zero to a maximum, (pseudo) steady state, value in approximately 150-200 hours. As would be expected, the oxygen-limited case showed higher utilization rates as higher growth rates would be allowed by the higher glucose concentrations.

Detachment Rates. Cellular detachment rate as a function of time is shown in Figure 6. As in the case of the substrate utilization rates, the detachment rates increased from zero at time zero and to a maximum, steady state value within 150-200 hours.

Note that for both the detachment and substrate loading rates the difference between the average values for the high and low glucose loading rate experiments differed by approximately the same factor, 5-7. This implied a proportionality between glucose utilization rates and detachment rates. A similar proportionality was seen in Peyton's work (1992) where the factor was that of approximately 10.

Figure 7 plots detachment rate as a function of glucose utilization rate. The units on the detachment rate were converted from cells m^{-2} h^{-1} to gCC m^{-2} h^{-1} by the conversion factor 1.46×10^{13} cells gCC^{-1} (determined by Peyton (1992) during similar experiments in an RABR). This plot includes transient and steady state data as was justified by the order

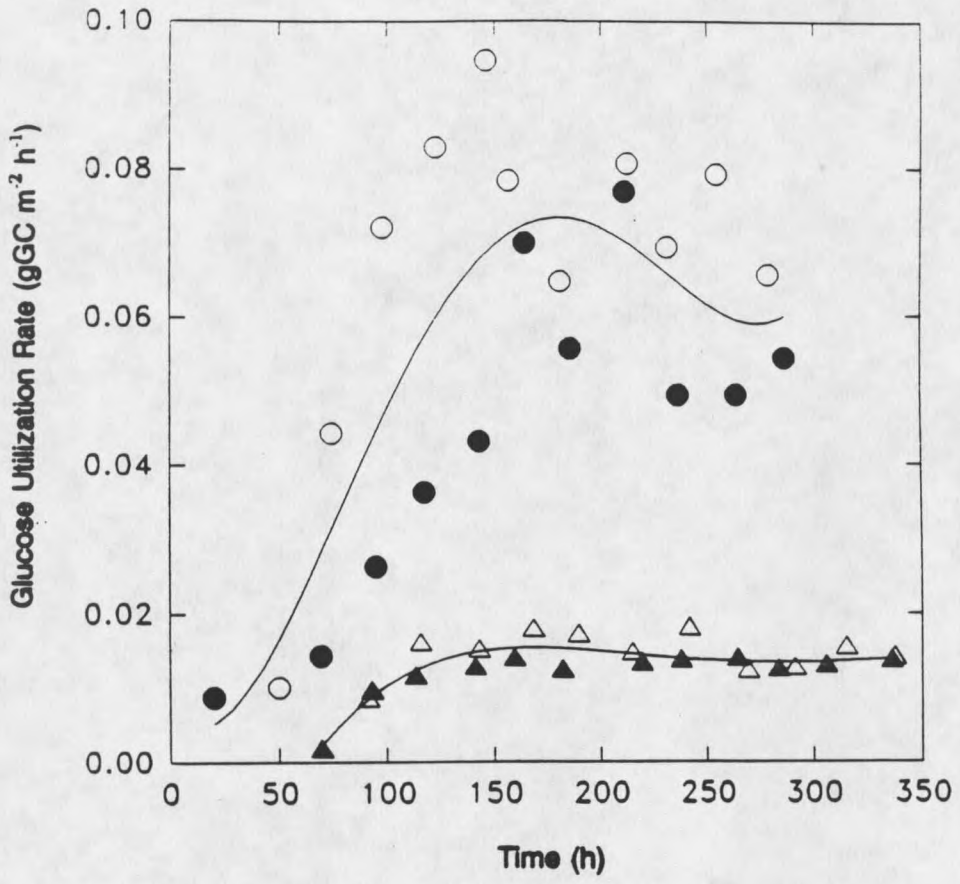

Figure 5. Glucose utilization rate vs. time. Circles indicate inlet glucose concentration of 18 g m^{-3}. Triangles indicate inlet glucose concentration of 2 g m^{-3}. Regression lines added to highlight trends.

of magnitude analysis discussed earlier.

If the reactor is assumed to operate as a differential reactor, mass balances predict detachment rates will correlate linearly with glucose loading rate (Peyton 1992). The line represents a linear regression of the data. The correlation coefficient, r^2, is equal to 0.53. While the goodness of fit indicated by the correlation coefficient is poor, there is a definite increase in detachment rate for an increase in glucose utilization rate.

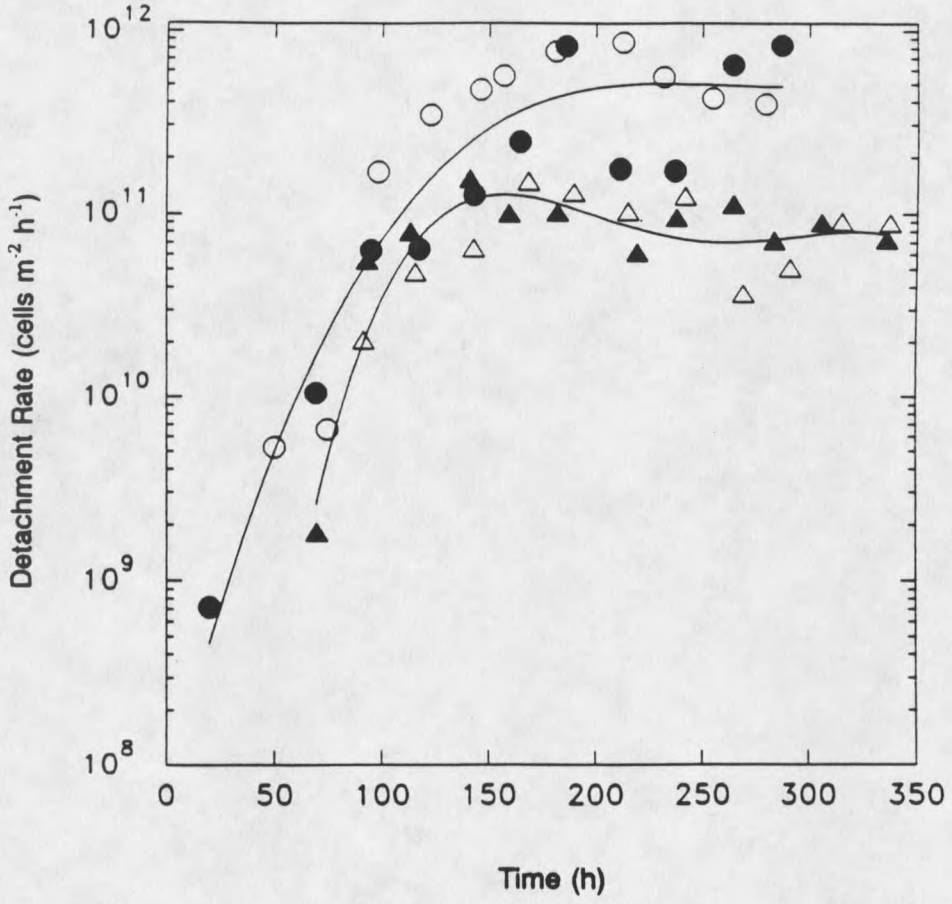

Figure 6. Cellular detachment rates vs. time. Circles indicate inlet glucose concentration of 18 g m^{-3}. Triangles indicate inlet glucose concentration of 2 g m^{-3}. Regression lines added to highlight trends.

Differential reactor theory also states that the slope of the line will be the yield of cell carbon from glucose (Peyton 1992). Based on the slope, a yield of 0.45 ± 0.06 gCC gGC^{-1} was calculated. This value is slightly higher than the value of 0.34 gCC gGC^{-1} reported by Characklis (1990) and the value of 0.182 gCC gGC^{-1} reported by Peyton (1991), both for Pseudomonas aeruginosa grown in RABRs. The lines predicted by the yields of Peyton and Characklis (lines b and c, respectively) do, however, fall within the scatter of data. It should be noted that the conversion factor used to calculate cell

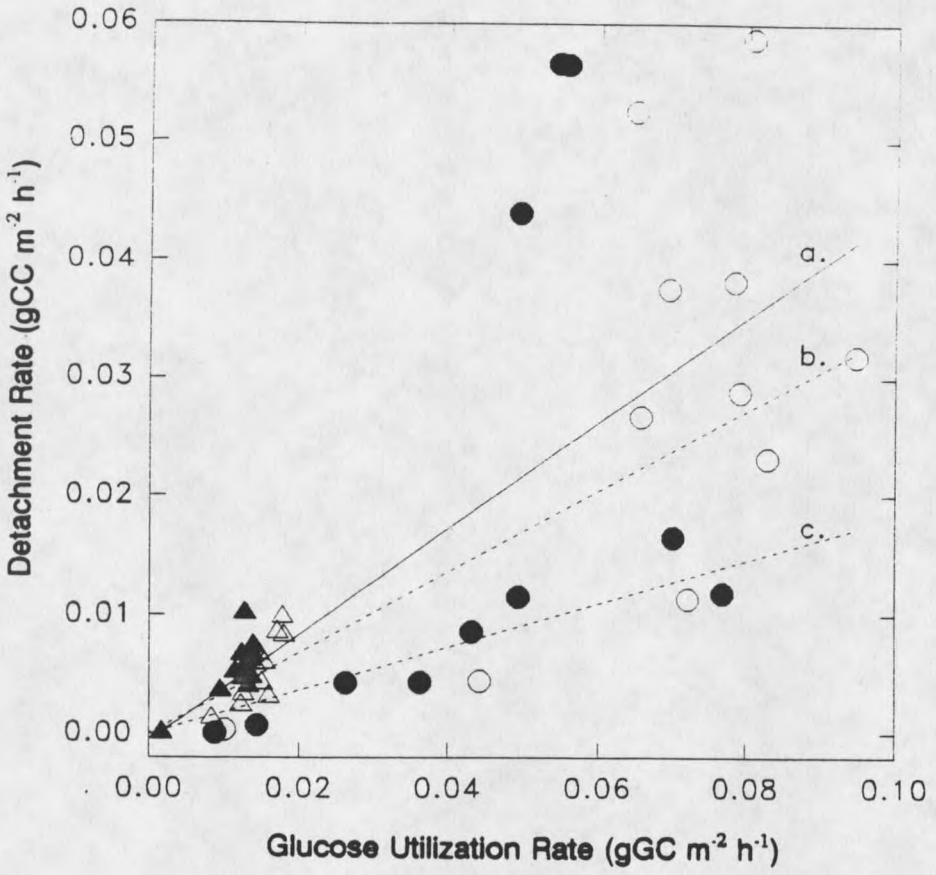

Figure 7. Detachment rate vs. glucose utilization rate. Circles indicate inlet glucose concentration of 18 g m^{-3}. Triangles indicate inlet glucose concentration of 2 g m^{-3}. Solid line (a) is linear regression of data indicating a yield (slope) of 0.45 gCC gGC^{-1}. Dashed lines, b and c, indicate yields of Peyton and Characklis, 0.34 and 0.182 gCC gGC^{-1}, respectively.

carbon from cell counts greatly affects the yield.

As is the case with most data from biological systems, the data presented here was quite noisy. Noise in the detachment rate data was at least in part due to the inherent error in cell counting. However, the glucose measurements (a very precise

procedure) also showed a high degree of variability, especially at the high glucose loading rate. This lead to the conclusion that the noise was partially due to a random or chaotic fluctuation of the system. Sloughing may have been partially responsible as it could produce the observed results.

Pressure Drop

The pressure drop data for both experiments is shown in Figure 8. The difference in the pressure drops between the two series of experiments was immense. Pressure drops across the reactor were viewed as an indirect measure of the mass of biofilm present. More biomass implied a larger pressure drop. Qualitatively, pressure drop agreed well with the microbead data, measured biomasses, and visual observations.

For the high glucose loading rate experiments, the pressure drop did not appear to reach any steady state value, even after a time period far exceeding the 150-200 hours required for either the glucose utilization or detachment rates to reach steady state. This was in agreement with later experiments by Thompson (1992) which indicated that for this system, bacteria, and experimental conditions; the pressure drop would not reach a pseudo-steady state until approximately 410 hours, at which time it would begin to oscillate. The oscillation in pressure drop was attributed to biomass sloughing from a part of the reactor. The related increase in porosity was assumed to translate into a decrease in pressure drop.

On the other hand, the pressure drop for the lower glucose loading rate experiments did reach a steady state. This was no doubt due to the inability of the

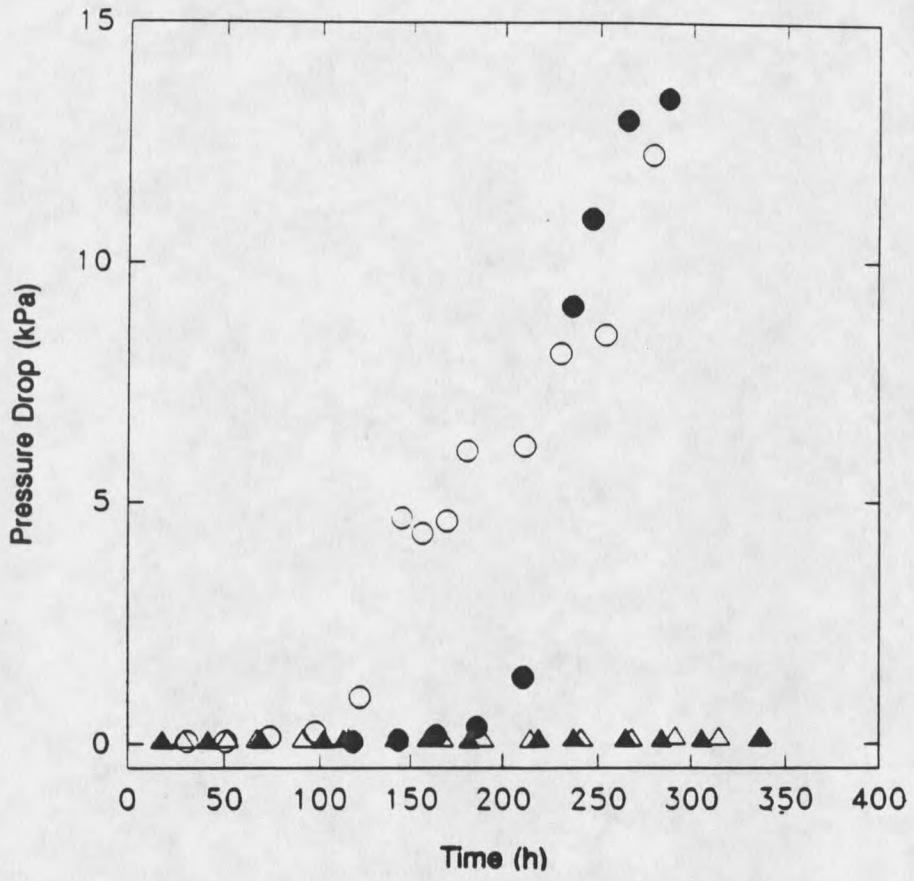

Figure 8. Pressure drop across the reactor vs. time. Circles indicate inlet glucose concentration of 18 g m^{-3}. Triangles indicate inlet glucose concentration of 2 g m^{-3}.

system to support the quantity of biomass seen in the reactor for the first series of runs. Less biomass implied less filtration of particulates, reducing the pressure drop even further.

Mass of Biological Accumulation in the System

The masses of bacteria and biological products removed from the reactor are listed in Table 2. The amount of biomass present in the system at high glucose loading rates was approximately seven times higher than the mass of material in the reactor at the low glucose loading rate.

Table 2. Total mass (g) of biofilm present in the reactor.

	Glucose Loading Rate	
	High	Low
Run 1	0.49	0.055
Run 2	0.28	--
Average	0.38	0.055

If, for the high glucose loading rate experiments, it is assumed that all pore spaces in the reactor were completely filled with bacteria and EPS, the density of the biofilm can be calculated as 34.8 kg m^{-3} and 20.0 kg m^{-3} for runs 1 and 2 respectively. These densities fall within reported values (Christensen and Characklis, 1990). The assumption of completely filled pores was verified by measuring the thickness of the film on the beads adjacent to the reactor wall at several locations. For these runs, the biomass completely spanned the pore space. At the low glucose loading rates, the density calculation could not be performed because the thickness of the biofilm was not measurable (<10μm).

Tracer Studies

The tracer studies for the first run of the high glucose loading rate experiment were unsuccessful due to equipment limitations. To correct the problems, an adjustable voltage offset was added to the electronics following the conductivity probe; a new data acquisition board capable of reading a broader range of voltages was added to the computer; and the reactor design was modified to allow for aseptic insertion and removal of probes to allow for daily calibration. The results from the second run of the high glucose loading rate series are shown in Figure 9. Other related, calculated quantities are shown in Table 3.

For the high glucose loading rate experiments, the effect of the biological accumulation on the residence time curves was immense. At 32 hours, the influent and effluent peaks were approximately the same height and shape. This indicated little, if any, dispersion. The breakthrough time of the response curve at 32 hours was still long, 24 seconds.

By 158 and 184 hours, the effluent peak was much shorter and wider than the influent peak, indicating a large degree of dispersion. The dispersion effect was further accentuated by the much shorter breakthrough times, 7 and 4 seconds for 158 and 184 hours, respectively. In both cases tailing (asymmetry) in the response curves was very prominent. The curves never completely returned to baseline.

The curves at 256 and 281 hours demonstrated the same shortened breakthrough times, 5 and 7 seconds, respectively. However, the curves returned to baseline. Not

Table 3. Summary of calculated values from stimulus-response curves.

Time (h)	t_b (s)	τ (s)	s (s^{-1})	Recovery (%)
18 g m^{-3} inlet glucose concentration, (Run 2)				
32	24	25	0.0146	127
158	7	30	0.0133	98
184	4	12	0.0143	100
256	5	23	0.0151	104
281	7	20	0.0147	92
2 g m^{-3} inlet glucose concentration, (Run 1)				
20	30	35	0.0151	96
71	29	33	0.0151	99
114	26	33	0.0160	93
220	31	37	0.0168	111
307	29	41	0.0223	98
2 g m^{-3} inlet glucose concentration, (Run 2)				
33	32	48	0.0158	100
92	30	26	0.0163	114
271	22	22	0.0157	93
317	25	23	0.0153	91
339	22	29	0.0155	108

t_b - breakthrough time (s)
τ - mean residence time (s)
s - weighting factor as calculated from equation 9 (s^{-1})

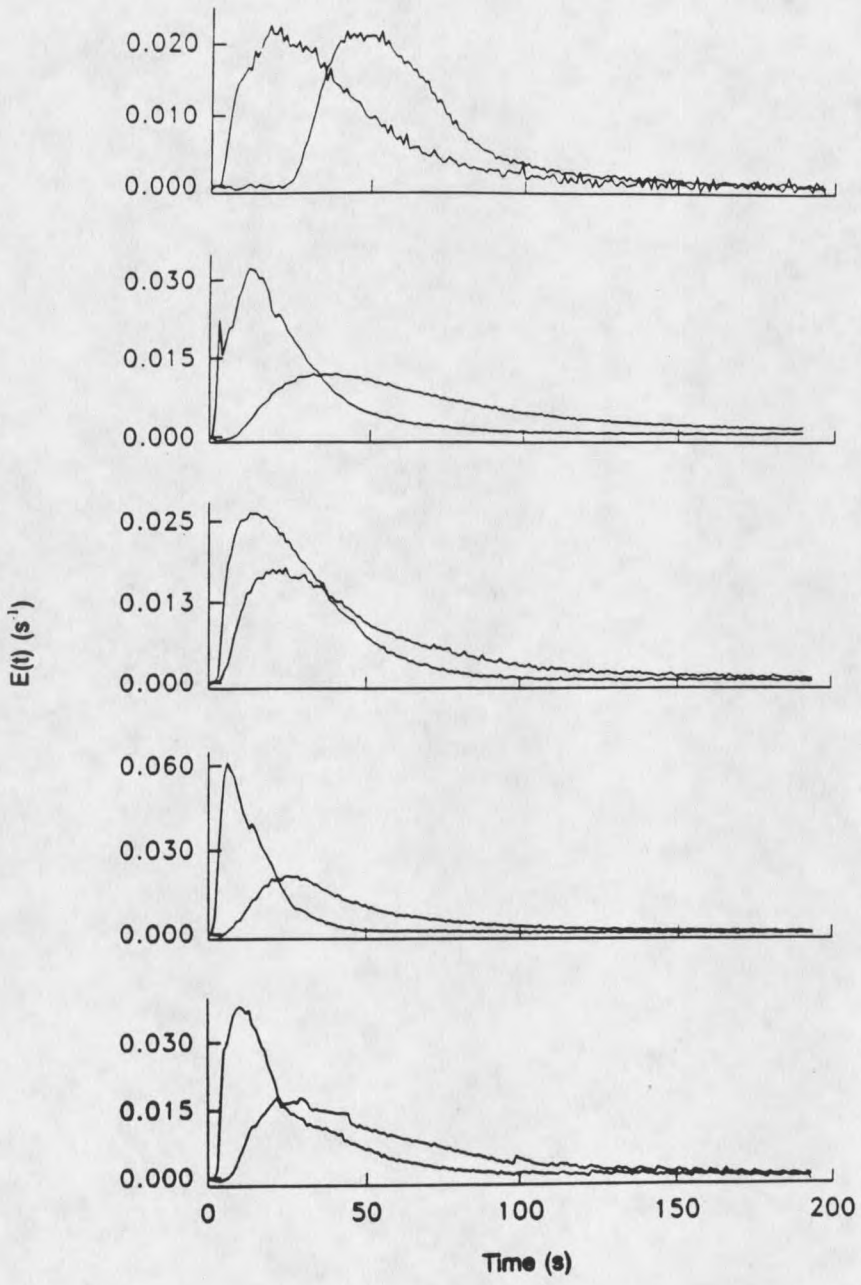

Figure 9. Time series of stimulus-response curves for second run of high glucose loading rate experiment. From top to bottom, times of experimental readings were 32, 158, 184, 256, and 281 hours from the start of the experiment.

much difference in the qualitative shape of the curves was noticed when compared with the curves from 158 and 184 hours.

Residence times were somewhat inconclusive. The hydraulic residence time for the clean reactor can be calculated as approximately 22 seconds. Therefore, all the residence times were within reason and no trends were apparent.

Results from the low glucose experiments are shown in Figures 10 and 11. From these stimulus-response curves it was evident that dispersion was reduced when the glucose loading rate was lowered as shortening of the effluent peak height and widening of the effluent curves occurred to a much lesser degree. The proposition that less dispersion was occurring was further supported by the breakthrough times of the response curves. Whereas for high substrate loading rates the breakthrough times decreased significantly during the first part of the run, the breakthrough times for the low glucose loading rate runs remained nearly constant for the duration of each experiment.

The response curves for the low substrate loading rates also showed less tailing. All the curves returned to baseline. Mean residence times were again close to expected values. The first run of the second series had slightly higher, but more consistent, residence times than the second run. No conclusion could be drawn as to trends.

Weighting factors were relatively constant for all the calculations. This was expected as the time values which determined the factors were of the same order of magnitude.

The tracer studies accurately reflected the rate and extent of the accumulation of biomass in the porous media. When comparing the runs from the high and low glucose

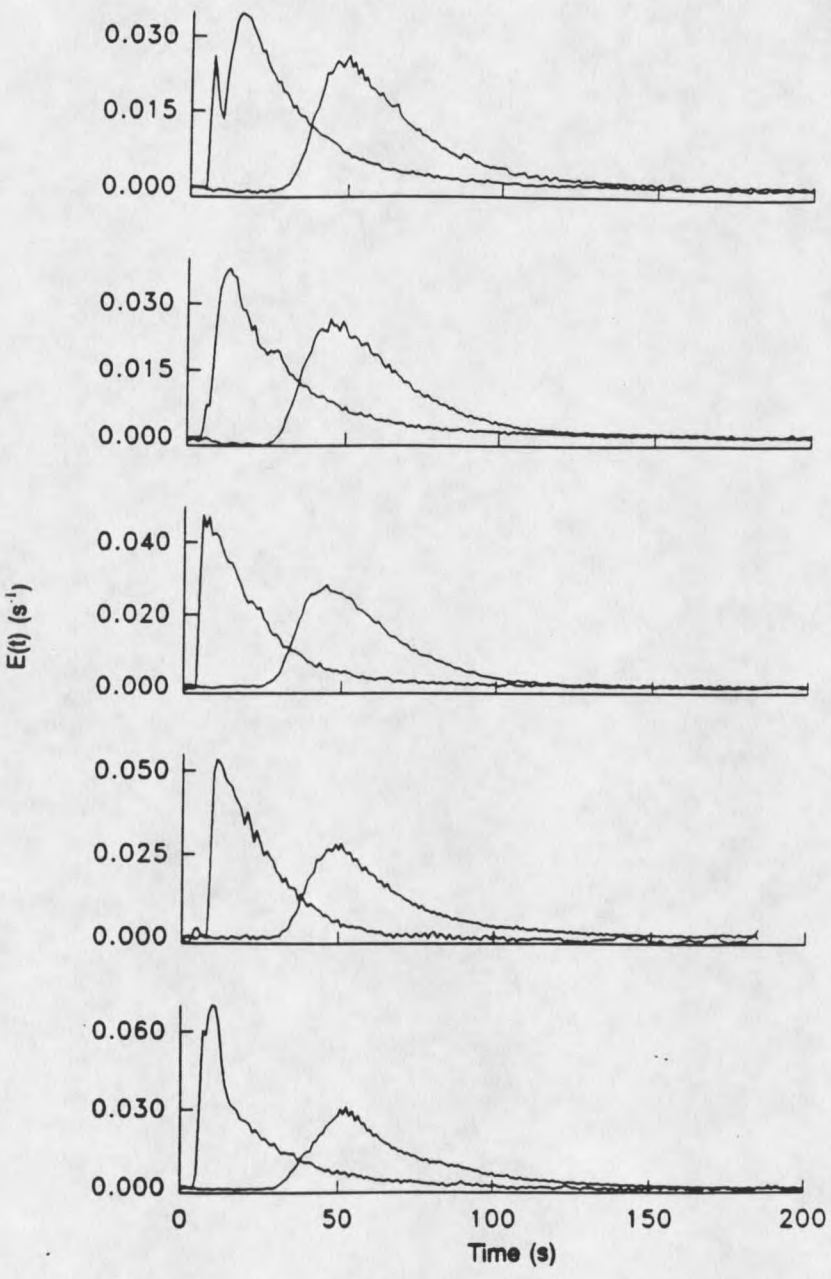

Figure 10. Time series of stimulus-response curves for first run of low glucose loading rate experiments. From top to bottom, times of reading were 20, 71, 114, 220, and 307 hours from the start of the experiment.

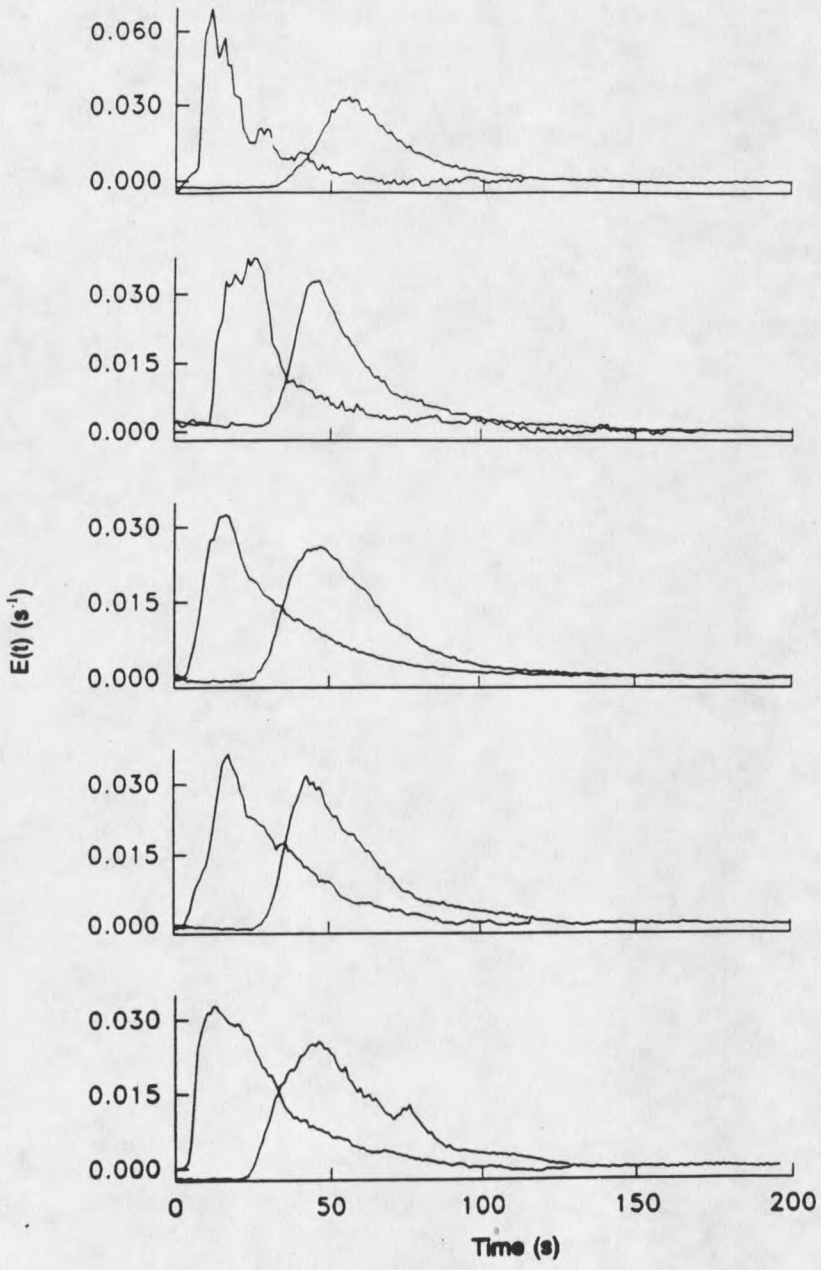

Figure 11. Time series curves for second run of the low glucose loading rate experiments. From top to bottom, times of readings were 33, 92, 271, 317, and 339 hours from the start of the experiment.

loading rates, the extent of dispersion was easily attributable to the differences in biomass concentration.

For the high substrate loading rate, the shorter peak height and tailing were due to the presence of biomass. As the bacteria and EPS accumulated in the reactor, channels and dead zones appeared. The shorter breakthrough times for the effluent curves reflected the channeling and/or dispersion effect. The tailing was the result of the dead zones and subsequent diffusion of the tracer into the bacteria/EPS matrix. It was hypothesized that when the concentration of tracer in the bulk liquid was high, tracer diffused into the dead zones. Once the concentration of the tracer in the bulk fluid was lower than the concentration in the dead zones, the tracer diffused back into the bulk fluid. This slow leaching of low concentrations of tracer from the biofilm into the bulk fluid was responsible for the tailing.

It is also proposed that dead zones were present on at least two scales. First, on the macroscale, entire sections of the reactor were excluded from flow due to pore plugging from upstream bacteria. Second, on the microscale, water trapped within the sponge-like structure of the biomass (Marshall and Characklis, 1986) was also excluded from bulk flow. Flow velocities in these regions, if non-zero, were very low.

For the runs with low glucose loading rates, the lack of biomass in the reactor was evident. The relative heights of the influent and effluent peaks were much more consistent throughout the experiment and the tailing phenomena was diminished. The symmetry of the curves indicated very few dead zones and channels. The breakthrough times of the effluent curves for the duration of the run were much closer to that of the first day when the reactor was essentially clean.

If the averages of the mean residence times are examined for each run, the low substrate loading experiments showed an increase in residence time over that of the expected hydraulic residence time. This may be due to the presence of a thin biofilm into which the tracer diffused. The film, however, was not thick enough to cause noticeable channeling. The tracer was retarded, but not significantly accelerated. This indicated that hydraulic and tracer residence times were not comparable. The residence time of substrate in the system may have been longer than the liquid residence time.

It is forwarded that the "open" pore model (Taylor and Jaffe, 1990) was the more accurate description of the system. The model predicts channels that lessen the tortuosity and length of the flow path. These effects were seen in the breakthrough times of the high glucose loading rate experiment. Furthermore, the open pore model was consistent with the recorded dispersivities. The proposition that tailing was due to tracer diffusion into the film required an a priori assumption that a bulk fluid/biofilm interface existed. The existence of such an interface was supported by the open pore model.

If the reactor were completely filled, such as the closed pore model would suggest, dispersion would have been much more symmetric. No time would have been needed for diffusion of the tracer into and out of the film. Dispersion effects would have been due to the mechanical mixing induced by the physical presence of the media and biofilm. This phenomena of mechanical mixing was much less pronounced than that of the diffusion-based dispersion as can be seen by comparing the stimulus-response curves of the low glucose loading rate runs (nearly clean reactors) with that of the high glucose loading rate runs (a nearly plugged reactor).

CONCLUSIONS

1) Data from the microbead experiments demonstrated that bacteria could penetrate the porous medium even after a significant biofilm had been established. However, high biomass concentrations in the media did increase filtration.

2) Detachment rates demonstrated a weak linear dependence on substrate utilization rates. The calculated yield for this experiment was slightly higher than the yields of Peyton (1992) and Characklis (1990) for RABRs. However, the detachment rates predicted by Peyton and Characklis did fall within the data presented.

3) The stimulus-response studies demonstrated the dramatic effect that the accumulation of biomass had on the flow of dissolved components through the reactor. Dispersion increased rapidly with increasing biomass concentration.

4) The "open" pore model (Taylor and Jaffe, 1990) was the more accurate description of the system. Breakthrough times and tailing supported the existence of channels in the form of small parallel conduits.

5) Finally, tracer residence times were longer than expected for the low glucose loading rate runs. This was proposed to be the result of diffusion of the tracer into a thin film. As not enough biomass was present to induce channeling, the tracer was retarded, but never accelerated. It was concluded that hydraulic residence times, which are commonly used in modelling, may not be representative of substrate residence times.

RECOMMENDATIONS

1) Further studies should be performed to better quantify the relationship between detachment rate and glucose utilization rate. This is especially important if a linear relationship is to be used for modelling purposes.

2) In future stimulus-response studies, the hydraulic residence time of the reactor should be increased. A longer hydraulic residence time would require the method of analysis to account only for the response curve. The stimulus curve could be assumed to be a perfect pulse (Dirac delta function). Less experimental error would be expected.

3) Future stimulus-response studies should be performed with a tracer which has no background level in the system. This may also provide less noise in the data.

4) If possible, a tracer more representative of the bulk fluid should be found. This would allow for a comparison between hydraulic and chemical specie residence times.

NOMENCLATURE

A	Area (L^2)
C	Concentration of tracer ($M\ L^{-3}$)
CC	Cellular carbon
GC	Glucose carbon
j	Index number
n	Number of data points
k_{ave}	Average order of the moment
k_{max}	Maximum order of the moment
Q	Volumetric flow rate ($L^3\ t^{-1}$)
R_a	Attachment rate ($M\ L^{-2}\ t$)
R_d	Detachment rate ($M\ L^{-2}\ t$)
s	Weighting factor (t^{-1})
Se	Effluent substrate concentration ($M\ L^{-3}$)
Si	Influent substrate concentration ($M\ L^{-3}$)
t	Time (t)
$\bar{t}$	First moment about the origin, residence time (t)
t_D	Time delay between stimulus and response curves (t)
V	Volume (L^3)
x	Distance from reactor inlet (L)
X	Cell concentration ($M\ L^{-3}$)
X_e	Effluent cell concentration ($M\ L^{-3}$)
X_i	Influent cell concentration ($M\ L^{-3}$)

Greek

Δt	Time between current and previous data point (t)
μ	Maximum specific growth rate (t^{-1})
τ	Mean residence time of system (t)

LITERATURE CITED

Abedeen, F., "Macroscopic Observations of Hydrodynamics and Pseudomonas aeruginosa Biofilm Processes in a Porous Media Reactor", 1990, Unpublished Masters Thesis, Montana State University.

Anderssen, A.S. and E.T. White, "Parameter Estimation by the Weighted Moments Method", Chemical Engineering Science, 1971, Vol. 26, pp. 1203-1221.

Anselme, M.J., and D.W. Tedder, "Characteristics of Immobilized Yeast Reactors Producing Ethanol from Glucose", Biotechnology and Bioengineering, 1987, Vol. 30, pp. 736-745.

Bryers, J.D., and W.G. Characklis, "Biofilms in Wastewater Treatment", in W.G. Characklis and K.C. Marshall (eds.), Biofilms, © 1990, John Wiley & Sons Inc., New York, NY, pp. 671-696.

Chang, H.T., and B.E. Rittmann, "Comparative Study of Biofilm Shear Loss on Different Adsorptive Media", Journal WPCF, 1988, Vol. 60, No. 3, pp. 362-368.

Chang, H.T., and B.E. Rittmann, "Mathematical Modeling of Biofilm on Activated Carbon", Environmental Science and Technology, 1987, Vol. 21, No. 3, pp. 273-279.

Chang, H.T., B.E. Rittmann, D. Amar, R. Heim, O. Ehlinger, and Y. Lesty, "Biofilm Detachment Mechanisms in a Liquid-Fluidized Bed", Biotechnology and Bioengineering, 1991, Vol. 38, pp. 499-506.

Characklis, W.G., "Kinetics of Microbial Transformations", in W.G. Characklis and K.C. Marshall (eds.), Biofilms, © 1990, John Wiley & Sons Inc., New York, pp. 251.

Christensen, B.E. and W.G. Characklis, "Physical and Chemical Properties of Biofilms", in W.G. Characklis and K.C. Marshall (eds.), Biofilms, © 1990, John Wiley & Sons Inc., New York, NY, pp. 110-111.

Cohen, Y., and A.B. Metzner, "Wall Effects in Laminar Flow of Fluids through Packed Beds", 1981, AICHE Journal, Vol. 27, No. 5, pp. 705-715.

Condoret, J.S., J.P. Riba, and H. Angelino, "Dispersion dans les Lits de Particules avec Ecoulement Pulse", The Canadian Journal of Chemical Engineering, 1989, Vol. 67, pp. 45-50.

Crawford, D.J., "Hydraulic Effects of Biofilm Accumulation in Simulated Porous Media Flow Systems", 1987, Unpublished Masters Thesis, Montana State University.

Danckwerts, P.V., "Continuous Flow Systems, Distribution of Residence Times", Chemical Engineering Science, 1953, Vol. 2, pp. 1-11.

Danckwerts, P.V., Insights into Chemical Engineering, Pergamon Press, Oxford (NY), ©1981, pp. 217-218.

Drury, W.J., "Interactions of 1-μm Latex Microbeads", 1992, Unpublished Ph.D. Thesis, Montana State University.

Freeze, R.A., and J.A. Cherry, Groundwater, Prentice Hall Inc., Englewood Cliffs, © 1979, pp. 75-76.

Gannon, J.T., V.B. Manilal, and M Alexander, "Relationship between Cell Surface Properties and Transport of Bacteria through Soil", Applied and Environmental Microbiology, 1991, Vol. 57, No. 1, pp. 190-193.

Godia, F., C. Casas, and C. Sola, "Mathematical Modelization of a Packed-Bed Reactor Performance with Immobilized Yeast for Ethanol Fermentation", Biotechnology and Bioengineering, 1987, Vol. 30, pp. 836-843.

Gonzalez, G., C. Caminal, C. de Mas, and J. Lopez-Santin, "An Approach in Mathematical Modeling of an Upflow Packed-Bed Reactor for Enzymatic Hydrolysis of Wheat Straw", Biotechnology and Bioengineering, 1989, Vol. 34, pp. 242-251.

Griebe, T., "Experimentelle Untersuchungen zur Aggregatbildung", 1991, Unpublished Masters Thesis, University of Hamburg.

Guzy, S., G.M. Saidel, and N. Lotan, "Multimolecular Process in a Packed-Bed Immobilized Enzyme Reactor: Numerical Simulation and Back-Mixing Effects", Biotechnology Progress, 1990, Vol. 6, pp. 98-103.

Hamamci, H. and D.D.Y. Ryu, "Performance of Tapered Column Packed-Bed Bioreactor for Ethanol Production", Biotechnology and Bioengineering, 1987, Vol. 29, 994-1002.

Hamer, J.W., and C.B. Richenberg, "On-Line Optimization of a Packed-Bed Immobilized-Cell Reactor", AICHE Journal, 1988, Vol. 34, No. 4, pp. 626-632.

Howell, J.A., and B. Atkinson, "Sloughing of Microbial Film in Trickling Filters", Water Research, 1976, Vol. 10, pp. 307-315.

Johnson, K.R., R.W. Lundman, and M.A. Hamilton, "Efficient Sampling Designs for Microbial Processes: A Case Study", Submitted for publication 1992, Montana State University.

Keck, D.W., "Determination of Mass Diffusivities", 1987, Unpublished B.S. Thesis, Montana State University.

Kennedy, K.J., and R.L. Droste, "Startup of Anaerobic Downflow Stationary Fixed Film (DSFF) Reactors", Biotechnology and Bioengineering, 1985, Vol. 27, pp.1152-1165.

Lamb, D.E., F.S. Manning, R.H. Wilhelm, "Measurement of Concentration Fluctuations with an Electrical Conductivity Probe", 1960, AICHE Journal, Vol. 6, No. 4, pp. 682-685.

McCready, K.A., "Measurement of the Intensity of Concentration Turbulence in Inline Motionless Mixing Systems", 1977, Unpublished Ph.D. Thesis, Montana State University.

McKinley, V.L., J.W. Costerton, and D.C. White, "Microbial Biomass, Activity, and Community Structure of Water and Particulates Retrieved by Backflow from a Waterflood Injection Well", Applied and Environmental Microbiology, 1988, Vol. 54, No. 6, pp. 1383-1393.

Naor, P., and R. Shinnar, "Representation and Evaluation of Residence Time Distributions", I & EC Fundamentals, 1963, Vol. 2, No. 4, pp. 278-286.

Ostergaard, K., and M.L. Michelsen, "On the Use of the Imperfect Tracer Pulse Method for Determination of Hold-Up and Axial Mixing", The Canadian Journal of Chemical Engineering, 1969, Vol. 47, pp. 107-112.

Peyton, B.M., "Kinetics of Biofilm Detachment", 1992, Unpublished Ph.D. Thesis, Montana State University.

Raiders, A.R., R.M. Knapp, and M.J. McInerney, "Microbial Selective Plugging and Enhanced Oil Recovery", Journal of Industrial Microbiology, 1989, Vol. 4, pp. 215-230.

Rittmann, B.E., "The Effect of Shear Stress on Biofilm Loss Rate", Biotechnology and Bioengineering, 1982, Vol. 24, pp. 501-506.

Rittmann, B.E., and P.L. McCarty, "Model of Steady-State-Biofilm Kinetics", Biotechnology and Bioengineering, 1980, Vol. 22, pp. 2343-2357.

Rittmann, B.E., and S.A. Wirtel, "Effect of Biofilm Accumulation on Colloid Cohesion", Journal of Environmental Engineering, 1991, Vol. 117, No. 5, pp. 692-695.

Sieble, M.A., "Binary Population Biofilms", 1987, Unpublished Doctoral Thesis, Montana State University.

Speitel, G.E., and F.A. DiGiano, "Biofilm Shearing under Dynamic Conditions", Journal of Environmental Engineering, 1987, Vol. 113, No. 3, pp. 464-475.

Sprouse, G., and B.E. Rittmann, "Colloid Removal in Fluidized-Bed Biofilm Reactor", Journal of Enviromental Engineering, 1990, Vol. 116, No. 2, pp. 314-329.

Strandberg, G.W., T.L. Donaldson, L.L. Farr, "Degradation of Trichloroethylene and trans-1,2,-Dichloroethylene by Methantrophic Consortium in a Fixed-Film, Packed Bed Bioreactor", Environmental Sciences and Technology, 1989, Vol. 23, No. 11, pp. 1422-1425.

Suschka, J., "Hydraulic Performance of Percolating Biological Filters and Consideration of Oxygen Transfer", Water Research, 1987, Vol. 21, No. 8, pp. 865-873.

Swaine, D.E. and A.J. Daugulis, "Review of Liquid Mixing in Packed Bed Biological Reactors", Biotechnology Progress, 1988, Vol 4, No. 3, pp. 134-148.

Taylor, S.W., and P.R. Jaffe, "Biofilm Growth and the Related Changes in the Physical Properties of a Porous Medium, 1. Experimental Investigation", Water Resources Research, 1990, Vol. 26, No. 9, pp. 2153-2159.

Taylor, S.W., and P.R. Jaffe, "Biofilm Growth and the Related Changes in the Physical Properties of a Porous Medium, 2. Permeability", Water Resources Research, 1990, Vol. 26, No. 9, pp. 2161-2169.

Taylor, S.W., and P.R. Jaffe, "Biofilm Growth and the Related Changes in the Physical Properties of a Porous Medium, 3. Dispersivity and Model Verification", Water Resources Research, 1990, Vol. 26, No. 9, pp. 2171-2180.

Taylor, S.W., and P.R. Jaffe, "Substrate and Biomass Transport in a Porous Medium", Water Resources Research, 1990, Vol. 26 No. 9, pp. 2181-2194.

Thompson, S., "Determination of Cellular Detachment Rate from a Porous Media Biofilm over 21 Days", 1992, Unpublished REU Summer Research Project, Montana State University.

Trulear, M.G., and W.G. Characklis, "Dynamics of Biofilm Processes", Journal of the Water Pollution Control Federation, 1982, Vol. 54, No. 9, pp. 1288-1310.

Updegraff, D.M., "Early Research on Microbial Enhanced Oil Recovery", Developments in Industrial Microbiology, 1990, Vol. 31 (Journal of Industrial Microbiology, Supplement No. 5), pp. 135-142.

APPENDICES

APPENDIX A

Raw Data

High Glucose Loading Rate - Run 1

Table 4. Concentration of Glucose in the Bulk Liquid.

Time (hours)	Mean Glucose Concentration ± Standard Deviation Influent (mg/l)	Effluent (mg/l)
20.1	24.8 ± 8.0	23.4 ± 0.1
44.7	26.3 ± 7.8	29.5 ± 10.9
69.4	30.6 ± 8.6	28.3 ± 0.2
95.1	27.8 ± 0.1	23.6 ± 6.7
117.6	24.0 ± 6.2	18.2 ± 0.2
143.2	17.1 ± 0.1	10.2 ± 0.0
164.4	19.9 ± 0.1	8.7 ± 0.1
186.0	17.8 ± 0.0	8.9 ± 0.0
211.0	16.1 ± 0.1	3.8 ± 0.1
236.9	17.0 ± 0.1	9.1 ± 2.0
264.9	20.1 ± 0.2	12.2 ± 4.0
287.1	18.7 ± 0.1	10.0 ± 0.0
309.1	41.5 ± 0.9	27.2 ± 9.1

Table 5. Concentration of Cells in the Bulk Liquid.

Time (hours)	Mean Cell Concentration ± Standard Deviation Influent (10^5 cells/ml)	Effluent (10^6 cells/ml)
20.1	0.0 ± 0.0	0.0457 ± 0.0431
44.7	0.0976 ± 0.171	0.0201 ± 0.0284
69.4	0.0854 ± 0.100	0.676 ± 0.193
95.1	0.535 ± 0.321	0.0537 ± 0.0322
117.6	0.244 ± 0.153	4.02 ± 0.571
143.2	0.639 ± 0.406	4.15 ± 1.42
164.4	5.42 ± 1.60	8.56 ± 2.39
186.0	2.59 ± 0.746	15.7 ± 5.83
210.0	1.73 ± 0.643	53.0 ± 12.3
236.9	6.54 ± 0.622	11.7 ± 3.34
264.9	10.8 ± 0.278	11.9 ± 3.17
287.1	18.7 ± 1.53	43.0 ± 13.1
309.1	7.88 ± 1.43	53.7 ± 21.5

Table 6. Pressure Drop Across Reactor as a Function of Time.

Time (hours)	Pressure Drop (kPa)
118.0	0.049
143.0	0.078
163.9	0.177
185.8	0.358
210.5	1.393
236.6	9.071
246.6	10.895
264.5	12.954
286.5	13.415
308.8	22.915

High Glucose Loading Rate - Run 2

Table 7. Concentration of Glucose in the Bulk Liquid.

Time (hours)	Mean Glucose Concentration ± Standard Deviation					
	Influent (mg/l)			Effluent (mg/l)		
29.4	19.62	±	0.43	19.63	±	0.35
49.9	20.04	±	0.48	18.44	±	0.26
74.4	19.99	±	0.21	12.95	±	0.80
98.3	19.85	±	0.46	8.38	±	0.49
122.7	18.82	±	2.07	5.65	±	1.43
145.9	19.90	±	0.41	4.85	±	0.02
156.8	15.55	±	1.35	3.10	±	0.12
181.2	14.08	±	2.06	3.79	±	0.44
212.4	15.86	±	1.34	3.05	±	0.36
231.3	14.92	±	1.29	3.88	±	0.18
254.6	16.92	±	2.00	4.33	±	0.25
279.4	15.30	±	0.11	4.86	±	0.61

Table 8. Concentration of Cells in the Bulk Liquid.

Time (hours)	Mean Cell Concentration ± Standard Deviation	
	Influent (10^5 cells/ml)	Effluent (10^6 cells/ml)
29.4	0.616 ± 0.460	0.282 ± 0.0732
49.9	1.62 ± 0.612	0.494 ± 0.158
74.4	7.14 ± 3.04	4.86 ± 1.43
98.3	2.71 ± 0.970	10.8 ± 3.64
122.7	4.13 ± 1.31	22.0 ± 4.99
145.9	9.09 ± 2.91	30.5 ± 5.68
156.8	6.81 ± 1.92	36.2 ± 10.3
181.2	13.8 ± 3.26	50.2 ± 11.8
212.4	19.6 ± 6.45	56.5 ± 15.4
231.3	50.5 ± 6.23	40.0 ± 10.0
254.6	18.2 ± 4.74	28.6 ± 6.31
279.4	17.7 ± 3.80	26.5 ± 5.89

Table 9. Pressure Drop Across Reactor as a Function of Time.

Time (hours)	Pressure Drop (kPa)
30.4	0.059
50.7	0.059
73.8	0.147
97.3	0.255
121.8	0.971
144.9	4.677
156.1	4.354
169.5	4.609
180.5	6.060
211.7	6.168
230.5	8.100
253.9	8.482
278.7	12.238

Low Glucose Loading Rate - Run 1

Table 10. Concentration of Glucose in the Bulk Liquid.

Time (hours)	Mean Glucose Concentration ± Standard Deviation Influent (mg/l)	Effluent (mg/l)
17.7	2.33 ± 0.05	2.86 ± 0.05
42.7	2.30 ± 0.11	2.30 ± 0.00
69.6	2.18 ± 0.05	1.92 ± 0.00
93.1	2.22 ± 0.05	0.72 ± 0.00
113.3	2.29 ± 0.05	0.47 ± 0.05
141.1	2.26 ± 0.05	0.24 ± 0.05
159.5	2.41 ± 0.05	0.21 ± 0.00
182.1	2.32 ± 0.20	0.37 ± 0.00
219.2	2.50 ± 0.05	0.40 ± 0.05
237.6	2.60 ± 0.00	0.44 ± 0.00
264.4	2.41 ± 0.05	0.21 ± 0.00
283.8	2.26 ± 0.05	0.28 ± 0.00
305.9	2.60 ± 0.10	0.54 ± 0.25
336.0	2.60 ± 0.10	0.44 ± 0.00

Table 11. Concentration of Cells in the Bulk Liquid.

Time (hours)	Mean Cell Concentration ± Standard Deviation Influent (10^5 cells/ml)	Effluent (10^5 cells/ml)
17.7	0.405 ± 0.267	0.877 ± 0.332
42.7	0.207 ± 0.077	0.445 ± 0.488
69.6	0.831 ± 0.906	1.95 ± 0.339
93.1	0.809 ± 0.152	34.9 ± 5.02
113.3	0.766 ± 0.189	49.7 ± 7.47
141.1	1.55 ± 0.722	96.1 ± 18.0
159.5	2.13 ± 0.327	63.8 ± 19.6
182.1	2.71 ± 0.888	65.3 ± 14.6
219.2	2.24 ± 0.766	40.1 ± 11.1
237.6	1.99 ± 0.850	60.8 ± 9.12
264.4	10.3 ± 5.88	79.5 ± 13.1
283.8	2.02 ± 1.01	46.1 ± 14.4
305.9	2.63 ± 1.66	57.8 ± 8.11
336.0	1.72 ± 0.515	46.6 ± 11.8

Table 12. Pressure Drop Across Reactor as a Function of Time.

Time (hours)	Pressure Drop (kPa)
17.4	0.049
41.5	0.049
69.1	0.059
102.1	0.069
113.0	0.078
140.9	0.088
159.1	0.088
181.8	0.069
218.9	0.088
237.3	0.098
264.2	0.088
283.5	0.088
305.6	0.088
335.8	0.098

Low Glucose Loading Rate - Run 2

Table 13. Concentration of Glucose in the Bulk Liquid.

Time (hours)	Mean Glucose Concentration ± Standard Deviation Influent (mg/l)			Effluent (mg/l)		
32.4	2.57	±	0.05	2.90	±	0.13
52.0	2.47	±	0.09	2.66	±	0.05
67.6	2.45	±	0.02	2.53	±	0.03
91.4	2.74	±	0.05	1.41	±	0.02
115.7	2.75	±	0.08	0.23	±	0.03
143.0	2.75	±	0.03	0.38	±	0.02
168.6	3.18	±	0.00	0.36	±	0.05
189.7	2.79	±	0.02	0.08	±	0.03
214.9	2.71	±	0.00	0.39	±	0.00
241.7	3.02	±	0.02	0.17	±	0.00
269.5	2.35	±	0.18	0.41	±	0.02
291.5	2.39	±	0.03	0.39	±	0.05
315.3	2.52	±	0.02	0.08	±	0.03
337.4	2.47	±	0.05	0.25	±	0.05

Table 14. Concentration of Cells in the Bulk Liquid.

Time (hours)	Mean Cell Concentration ± Standard Deviation Influent (10^5 cells/ml)	Effluent (10^5 cells/ml)
32.4	1.28 ± 0.359	1.81 ± 0.567
52.0	0.577 ± 0.672	2.26 ± 0.619
67.6	0.269 ± 0.178	0.569 ± 0.161
91.4	0.896 ± 0.361	13.5 ± 4.68
115.7	0.619 ± 0.153	30.1 ± 4.92
143.0	0.660 ± 0.337	40.6 ± 5.49
168.6	0.511 ± 0.336	92.1 ± 96.0
189.7	0.546 ± 0.424	80.1 ± 15.5
214.9	1.03 ± 0.319	64.0 ± 17.0
241.7	1.02 ± 0.470	77.9 ± 17.7
269.5	0.506 ± 0.312	23.2 ± 12.8
291.5	0.640 ± 0.361	32.0 ± 13.2
315.3	0.697 ± 0.331	56.4 ± 12.7
337.4	1.36 ± 0.597	56.5 ± 21.2

Table 15. Pressure Drop Across Reactor as a Function of Time.

Time (hours)	Pressure Drop (kPa)
28.3	0.069
51.8	0.078
67.2	0.078
91.1	0.078
115.4	0.088
142.7	0.088
167.5	0.088
189.3	0.088
214.6	0.078
241.3	0.098
267.5	0.098
291.3	0.137
315.0	0.127
336.7	0.127

APPENDIX B

Reactor Feed Composition

Table 16. Concentration of nutrients in reactor feed.

Nutrient	Concentration ($g\ m^{-3}$)
Glucose	18.0 or 2.0
Ammonium Chloride	7.2
Magnesium Sulfate • $7H_2O$	2.0
Calcium Chloride	1.0
Zinc Sulfate • 7 H_2O	0.100
Manganese Sulfate • H_2O	0.008
Copper Sulfate • 5 H_2O	0.002
Sodium Borate • 10 H_2O	0.001
Iron Sulfate • 7 H_2O	0.112
Aceto Nitrilic Acid	0.400
Sodium Phosphate (Na_2HPO_4)	213.0
Potassium Phosphate (KH_2PO_4)	204.0